SEMMELWEIS EGYETEM

DOKTORI ISKOLA

Ph.D. értekezések

3402.

VÁNCZA LÓRÁND

Onkológia

című program

Programvezető: Dr. Bödör Csaba, egyetemi tanár

Témavezetők: Dr. Kovalszky Ilona, egyetemi tanár és

Dr. Dezső Katalin, egyetemi tanár

SPOCK1 EXPRESSION IN LIVER REGENERATION, CIRRHOSIS AND HEPATOCELLULAR CARCINOMA

PhD thesis

Lóránd Váncza

Semmelweis University Doctoral School

Pathological and Oncological Division

Supervisor: Ilona Kovalszky MD, DSc

Katalin Dezső MD, PhD

Official reviewers: Judit Halász MD, PhD

Gertrud Forika MD, PhD

Head of the Complex Examination Committee: Anna Tompa, MD, D.Sc

Members of the Complex Examination Committee: Tibor Füle, Ph.D

Bálint Tegze, MD, Ph.D

Budapest

2026

TABEL OF CONTENT

List of Abbreviations

AFP	alpha-fetoprotein
AKT	protein kinase B
ALD	alcoholic liver disease
BrdU	bromodeoxyuridine
CDK1	cyclin-dependent kinase 1
cDNA	complementary deoxyribonucleic acid
CHD1L	chromodomain helicase DNA binding protein 1 like
CI	confidence interval
CK19	cytokeratin-19
CS	chondroitin sulfate
CTGF	connective tissue growth factor (),
CV	central vein
DAPI	4′,6-diamidino-2-phenylindole
DEN	diethylnitrosamine
DMEM	dulbecco's Modified Eagle Medium
EC	extracellular
ECM	extracellular matrix
EGF	epidermal growth factor
EGFR	epidermal growth factor receptor
ELISA	enzyme-linked immunosorbent assay
EMT	epithelial to mesenchymal transition
EpCAM	Epithelial cell adhesion molecule
F	forward
FBS	fetal bovine serum
FFPE	formalin-fixed paraffin-embedded
FGF	fibroblast growth factor
GAG	glycosaminoglycan
GAPDH	glyceraldehyde 3-phosphate dehydrogenase
HBV	hepatitis B-virus
HCC	hepatocellular carcinoma
HCV	hepatitis C-virus

HE	hematoxylin eosin
HE	hematoxylin and eosin
HGF	hepatocyte growth factor
HRP	horseradish peroxidase
HS	heparan sulfate
HSC	hepatic stellate cell
IHC	immunohistochemistry
KD	knock down
MASLD	metabolic dysfunction-associated steatotic liver disease
MMP	matrix metalloproteinases
mRNA	messenger ribonucleic acid
NSCLC	non-small cell lung cancer
ORF	open reading frame
PBS	phosphate-buffered saline
PBST	phosphate-buffered saline with Tween-20
PCR	polymerase chain reaction
PDGF	platelet-derived growth factor
PG	proteoglycans
PI3K	phosphoinositide 3-kinase
PV	portal vein
R	reverse
RNA	ribonucleic acid
RT-qPCR	quantitative reverse transcription polymerase chain reaction
SD	standard deviation
SFK	Src family kinases
SPARC	secreted protein acidic and rich in cysteine
SPOCK	Sparc/ osteonectin, cwcv, and kazal-like domains proteoglycan
TBST	tris-buffered saline containing Tween-20
TCGA	The Cancer Genome Atlas
TGF	transforming growth factor
TIMP	tissue inhibitor of metalloproteinases
UCP-1	uncoupling Protein 1

WES	Automated Western Blotting System
ZEB	zinc-finger E-box-binding homeobox

1. Introduction

Sparc/ osteonectin, cwcv, and kazal-like domains proteoglycan 1 (SPOCK1) is a chondroitin sulphate-heparan sulphate proteoglycan (CSHS-PG) that was first isolated and characterized from seminal plasma in 1992. The following year, it was cloned from human testicular complementary deoxyribonucleic acid (cDNA) libraries, leading Patrick M. et al. to propose the name testican (1,2). Since then, two other testican-like proteins have been identified the protein is now known as testican-1. Another name of the protein is Sparc/ osteonectin, cwcv, and kazal-like domains proteoglycan 1 reflecting its modular structure (3). It has recently attracted considerable interest because of its involvement in several types of cancer, but little is known about its role in the normal liver, in the controlled proliferation of the hepatocytes during liver regeneration or in liver cirrhosis and hepatocellular carcinoma (HCC). This study aims to elucidate the role of the SPOCK1 in these physiological and pathological processes of the liver.

1.1. Liver regeneration

Acute ingestion of toxins (e.g. acetaminophen), trauma and fulminant hepatitis can cause extensive parenchymal necrosis which initiates liver regeneration (4). The regulation of liver regeneration is a complex process and most of our knowledge originates from animal experiments.

The most widely used animal model for liver regeneration is the traditional partial hepatectomy, which consists of surgical removal of two-thirds of the liver mass in rodents (5). The most important signaling pathways identified are: (a) epidermal growth factor receptor (EGFR) signaling (ligands relevant to liver regeneration are epidermal growth factor (EGF), amphiregulin, transforming growth factor (TGF)α and heparin-binding EGF- like growth factor) and (b) hepatocyte growth factor (HGF)/MET (4). Within minutes after partial hepatectomy, urokinase type plasminogen activator initiates ECM remodeling mediated by plasminogen and metalloproteinases (6). The extracellular matrix (ECM) of the liver contains very high levels of HGF and matrix degradation produces active two-chain HGF, which stimulates hepatocytes to enter the cell cycle. Elimination of both EGFR and HGF/MET signaling pathways completely abolishes liver regeneration (7). Many auxiliary signals play an important role in regeneration such as

noradrenaline, bile acids, interleukin 6, insulin, serotonin, leptin and ablation of any of these signals can delay the recovery (4,7).

PGs have an important role in the restoration of normal liver structure. Undulating changes in the ribonucleic acid (RNA) expression of the syndecan-1, perlecan, syndecan-2, and decorin have been observed after partial hepatectomy in rats (8). For example, decorin peaked at 30 minutes, 24 hours and 96 hours, while perlecan peaked at 4 hours and 24 hours after partial hepatectomy. Syndecan-1 had oscillatory dynamic in the first 24 hours and syndecan-2 had decreasing levels throughout the period tested (8). Endocan is a circulating dermatan sulphate PG and its level decreases after partial hepatectomy in the liver with an increase in serum levels (9). There is currently no data on the involvement of SPOCK1 in the liver regeneration.

In human liver two distinct morphological patterns of regeneration have been distinguished after fulminant hepatic failure, depending on the cause and the extent of the parenchymal necrosis (10). (a) If significant viable parenchyma remains the surviving hepatocytes dedifferentiate, organize into acinar structures, and start to proliferate. Interestingly these hepatocytes begin to express the oncofetal marker alpha-fetoprotein (AFP) and glypican-3 which can be explained by hepatocyte dedifferentiation (10). So far there is no animal model which reliably reproduce the dedifferentiation, acinar arrangement and proliferation of the hepatocytes seen in this type of regeneration. (b) If the surviving parenchyma is negligible, the regeneration is accomplished by the progenitor cells (10). These cells are located in the proximal branches of the biliary three, in the canal of Hering and express the Epithelial cell adhesion molecule (EpCAM) marker. The liver progenitor cells are activated when hepatocytes fail to regenerate the liver (11). Prominent periportal ductular reaction is characteristic for this subtype of regeneration. Enlarged cells resembling hepatocyte morphology with pale eosinophilic cytoplasm, low cytokeratin 19 (CK19) and higher arginase-1 and hepatocyte nuclear factor 4 alpha expression appear at the distal portion of the ductules. The round clusters of hepatocytes form regenerative foci of variable size (10). The animal model of the progenitor cell mediated regeneration is the 2-acetylaminofluorene-partial hepatectomy model in rats. 2-acetylaminofluorene forms DNA adducts in hepatocytes inhibiting their proliferation and the regeneration is accomplished through the oval cells (liver progenitor cells in rats) (12).

1.2. Hepatocellular carcinoma

Primary liver cancer is the sixth most common neoplasm and the third leading cause of death worldwide with global incidence of 866 136 and mortality of 758 725 (13–15). The incidence varies widely worldwide, with the highest reported in Eastern Asia. HCC is the most common primary liver cancer representing 80% of the cases (16). The global epidemiology of HCC is changing due to the increasing incidence of metabolic dysfunction-associated steatotic liver disease (MASLD) and the decreasing prevalence of hepatitis B-virus (HBV) and hepatitis C-virus (HCV) related liver disease (15,16).

The strongest risk factor for HCC is chronic liver disease leading to cirrhosis (17). Cirrhosis is the diffuse nodular transformation of the liver after a long period of inflammation resulting in replacement of the normal liver parenchyma with fibrotic tissue and cirrhotic nodules (18). It starts with formation of porto-portal and porto-central fibrotic septa which divide the liver parenchyma. In response to the parenchymal extinction ductular progenitor cells differentiate and form round clusters of hepatocytes (19). The expanding regenerative nodules cannot reproduce the normal lobular structure of the liver, also they compress the hepatic veins leading to portal hypertension (20).

Cirrhosis of any etiology can promote hepatocarcinogenesis, and in 41.0% of the HCC cases occur in the setting of HBV infection, 28.5% in HCV infection, 18.4% in alcoholic liver disease, 6.8% in MASLD and in 5.3% in other less-common risk factors (16).

For surveillance, current guidelines recommend ultrasound-based examination with measurement of AFP levels every 6 months in patients with compensated cirrhosis (21). In non-cirrhotic patients biopsy and histopathological examination is always recommended for the diagnosis (22). In patients with previous diagnosis of HCC or with high risk of HCC (presence of cirrhosis, chronic HBV infection) a new hepatic nodule can be diagnosed as HCC based on contrast-enhanced imaging (multiphasic computed tomography, dynamic contrast-enhanced magnetic resonance imaging) and/or histopathological examination (22). Imaging-based diagnosis relies on vascular derangement occurring during hepatocarcinogenesis, resulting in changes in lesion appearance in the arterial-, portal venous-, or delayed phase. It presents as hyperenhancement in the arterial phase and wash-out on portal venous and/or delayed

phase. It has a sensitivity of 67% and a specificity of 93%, but the performance is lower in lesions smaller than 2 cm (23,24).

The most frequent morphological patterns observed in HCC are: steatohepatitic, trabecular, pseudoglandular, scirrhous, solid and macrotrabecular. Other features include lack of the portal triad, increased arteriolisation with unpaired arteries. Hepatocyte plates expand and the normal reticulin framework reduce (23,25).

The most frequent genetic alteration found in HCC was a telomerase reverse transcriptase promoter mutation, present in 65% of the cases. CTNNB1 mutation, identified in 40% of the cases, was associated with a well-differentiated phenotype, microtabecular or pseudoglandular pattern without inflammatory infiltrates. Low AFP expression, low cell proliferation rate were also characteristic (26). CTNNB1 mutation and TP53 mutations were mutually exclusive, the latter was found in 21% of the tumors and was associated with poor differentiation, high proliferation rate and frequent vascular invasion (26,27). The macrotrabecular-massive growth pattern is associated with TP53 mutations and this subtype correlates with poor prognosis and is a predictor of early and overall recurrence after surgical resection or radiofrequency ablation (28). Fibroblast growth factor (FGF)19 amplification is often seen in this entity, as well as high levels of AFP expression (26). The scirrhous subtype has a prominent fibrous stroma and is characterized by tuberous sclerosis complex1/2 mutation. The steatohepatitic subtype is typically well-differentiated and represents a less aggressive histological phenotype with a lack of satellite nodules. It is frequently associated with activation of the IL6/JAK/STAT signaling pathway (25). Fibrolamellar carcinoma is characterized by tumor cells with abundant eosinophilic cytoplasm and prominent nucleoli embedded in a dense fibrous stroma. Intracytoplasmic hyaline bodies are also common. This rare subtype predominantly affects young patients without cirrhosis. Recent studies have identified the DNAJB1-PRKACA fusion protein as the key genetic driver in fibrolamellar carcinoma. Currently, morpho-molecular subtyping of the HCC does not have a major impact on clinical decision making (25,29).

Surgical resection, organ transplantation and ablation are considered curative therapies for HCC. Liver resection is the recommended therapeutic option for patients with single HCC lesion and without cirrhosis (22). Liver resection also can be considered in cirrhotic

patients with single lesion, preserved liver function (Child-Pugh class A with total bilirubin <1 mg/dL; Model for End-Stage Liver Disease score <9) and absence of portal hypertension. Perioperative mortality is less than 5%, and postoperative decompensation rages between 10-12% (30). Liver transplantation provides the best long-term oncological outcome. For those who meet the Milan criteria, the 10 year survival rate after liver transplantation is 61.5% and the recurrence rate is 13.3% (31). Ablation induces necrosis of the tumor by temperature change or chemical agents. Radiofrequency ablation is the most commonly used, but microwave ablation, cryoablation or ethanol are also effective.

For patients with advanced unresectable HCC, atezolizumab (anti-programmed death-ligand 1) and bevacizumab (anti–vascular endothelial growth factor) became the standard of care and proved to be superior to Sorafenib (multikinase inhibitor) with overall survival at 12 months of 67.2% versus 54.6%, median progression free survival of 6.8 months versus 4.3 months (32).

1.3. Proteoglycans

A PG is a core protein covalently attached to glycosaminoglycan (GAG) chains. They are synthetized in the endoplasmic reticulum and Golgi. GAGs are repetitive sulphated disaccharide units comprising a galactose or uronic acid (glucuronic acid or iduronic acid) and an amino-monosaccharide (N-acetylglucosamine or N-acetylgalactosamine) (33,34). The variation in the monosaccharide and the presence or absence of the sulphation results in different categories of GAGs, such as CS, dermatan sulfate, keratan sulfate and HS/heparin. A variable number of GAGs can be attached to the core protein, hybrid PGs also carry more than one type of GAG chain. Based on their cellular localization PGs can be classified into intracellular, cell surface and extracellular groups. Generally, most HSPG are membrane type or intracellular PGs, whereas most CSPG are extracellularly localized (35,36).

PGs regulate the activity of several extracellular enzymes, interact with growth factors such as FGF, bone morphogenetic protein, Wnt proteins, insulin-like growth factor, and thus regulating signaling pathways (37). They can modulate the mechanical properties of the tissues by increasing ECM stiffness and bulkiness of the glycocalyx, promoting the malignant transformation (38). HSPGs also serve as binding site for viruses such as severe

acute respiratory syndrome coronavirus 2 (SARS-CoV-2) or HCV, thus facilitating their cellular entry (39,40).

GAG composition of the liver is altered in cancer. In HCC, CS levels increase 24 fold compared to normal liver, whereas HS level decreases during hepatocarcinogenesis, and this correlate with the differentiation status of HCC (41,42).

Under normal conditions, the liver contains predominantly HSPGs. One of the major HSPGs in the liver is syndecan-1, which is expressed on the basolateral surface of the hepatocytes and cholangiocytes. Its levels are elevated in cirrhotic livers particularly in cirrhosis of HCV etiology. Its high expression in HCC correlated with well differentiated phenotype and lack of extrahepatic metastasis (43). Moreover, HCC development is delayed in syndecan-1 transgenic mice in the diethylnitrosamine (DEN)- induced hepatocarcinogenesis model (44).

1.4. SPOCK1

SPOCK protein family consists of three proteoglycans: SPOCK1, SPOCK2 and SPOCK3. They show high homology and share several domains: N-terminal testican-specific domain, follistatin-like domain, extracellular calcium-binding domain, thyropin domain and domain V (45). SPOCK2 is detected mainly in brain, lung, adrenal gland and testes of mice and it plays a regulatory role in development of the central nervous system (46,47). SPOCK3 mRNA restricted to the brain in adult mice and is associated with protease inhibitory function (45,48).

The human SPOCK1 gene is located on chromosome 5q31.2 and consists of 11 exons (49). As a matricellular protein, SPOCK1 has an increased number of splice variants. The ENSEBL database includes ten human splice variants for SPOCK1, three of which encode potentially functional proteins (SPOCK1-201, SPOCK1-208, SPOCK1-203) (50,51).

SPOCK1 belongs to the ‘secreted protein acidic and rich in cysteine’ (SPARC) family. Beside SPOCK1, other members include SPARC, Hevin, SPOCK-2, and -3, SMOC-1 and -2, and FSTL-1. They share three domains: the signal peptide, follistatin-like domain and calcium binding domain. In addition to these, the SPOCK and SMOC proteins also share a tyropin domain homology. They are expressed during development, tissue repair

or in response to stress or injury (52,53). They play role in the regulation of connective tissue assembly and deposition, counter-adhesion, effects on extracellular protease activity, and modulation of growth factor/ cytokine signaling pathways (54).

1.4.1. Protein structure and predicted function

SPOCK1 encodes a protein precursor of 439 amino acids organized in modular structures (Figure 1A). The six identified domains are as follows (Figure 1B):

N-terminal hydrophobic signal sequence: contains a signal sequence at the amino terminal of the PG, which is characteristic for extracellular proteins (55). This ensures the insertion of the protein into the endoplasmic reticulum membrane during translation and directs the protein to the secretory pathway. The signal sequence is co-translationally cleaved from the protein between amino acids 21S and 22R. SPOCK1 has been shown to be secreted into the blood plasma, seminal plasma and cerebrospinal fluid (56,57).

N-terminal region: unique to testicans and not yet associated with any function.

Follistatin-like domain: encoded by exons 5 and 6. Consists of five disulfide bridges in the region between cysteine 86 and cysteine 182, three of which are located within the Kazal-like domain. It has been associated with serine protease inhibitory function (58).

The Extracellular (EC) calcium binding domain shares homology with the calcium binding domain of osteonectin, and consists of an EF-hand pair. In osteonectin, calcium binding promotes alpha-helical conformational changes and facilitates binding to multiple collagen types. Compared to the similar domain of osteonectin, the EC domain in SPOCK1 has more sequence deletions, significantly lower affinity for calcium and no evidence for collagen binding (59,60).

Thyropin domain homology covers the region between 310 and 379 amino acids encoded by exons 9 and 10. Is a cysteine rich module containing a type 1 thyroglobulin repeat with two highly conserved motifs (QC and CWCV). Thyropins are potent cysteine protease inhibitors, and studies have shown that SPOCK1 is a potent competitive inhibitor of the lysosomal cysteine protease, cathepsin L. (61,62).

Domain V: during the post-translational modification, GAG chains are linked to this carboxyl terminal domain. SPOCK1 carries both CS and HS (CS is dominant), in contrast to SPOCK2 and SPOCK3, which are pure HSPGs (45). This domain contains two serine

residues at positions 383 and 388, surrounded by specific sequence elements required for glycosylation (Ser-Gly) (2,63).

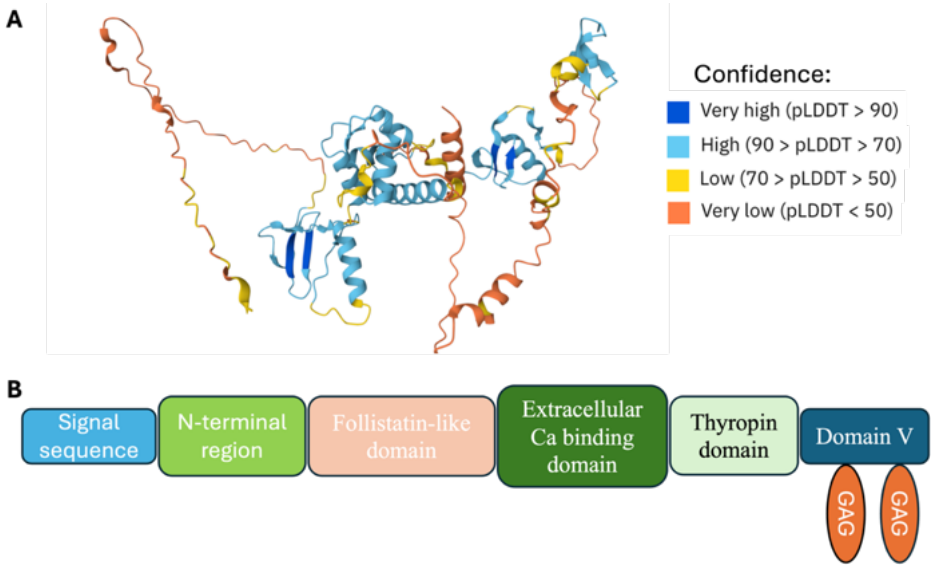

Figure 1. (A) SPOCK1 protein structure generated from AlphaFold Protein Structure Database (64,65). (B) Schematic representation of the modular structure of SPOCK1.

1.4.2. Physiological function and expression of SPOCK1

SPOCK1 messenger ribonucleic acid (mRNA) is highly expressed in the human brain (thalamus, nucleus accumbens, caudate nucleus and in the post synaptic regions of the hippocampal pyramidal cells) (66,67). It has also been detected in the heart, placenta, skeletal muscle, kidney, pancreas, spleen, thymus, prostate, testis, small intestine, colon, with reduced levels observed in the ovary (68).

The increase in SPOCK1 expression in mice during the embryonic period corresponds to the major steps in neuronal development, in areas active in cell proliferation, cell migration, axonal outgrowth and synaptogenesis (69).

Interestingly, SPOCK1 deficient mice did not show morphological and behavioral abnormalities and had normal life span (70). After cryo-injury of the brain SPOCK1 expression increases in the region surrounding the necrotic tissue. Its co-expression with FGF2 suggests a permissive role for regenerating axons in reactive astrocytes (71). This correlates with the fact that, in general mice deficient in matricellular protein result in mild phenotype, differences compared to wild type mice are only seen in response to injury or stress (54).

High expression of SPOCK1 was measured during adipocyte differentiation in the conditioned media in vitro, also recombinant SPOCK1 upregulated genes associated with adipocyte differentiation. SPOCK1-transgenic mice (SPOCK1 expressed under the cytomegalovirus enhancer element and chicken beta-actin promoter) showed increased maturation in epididymal and inguinal adipose tissues and SPOCK1 was highly expressed in adipose tissues of mice fed with high fat diet (72,73).

1.4.3. Genetic alteration

So far, only one spontaneous mutation in the human SPOCK1 gene was associated with a human phenotype. Whole exome sequencing has revealed a missense mutation on chromosome 5q31: c.239A>T (p.D80V). “Her features include intellectual disability with dyspraxia, dysarthria, partial agenesis of corpus callosum, prenatal onset microcephaly and atrial septal defect with aberrant subclavian artery”. Online predictive tools have suggested it as a deleterious mutation. No other genetic alteration has been identified that could be associated with her condition (74).

1.4.4. The role of SPOCK1 in cancer

Overexpression of the SPOCK1 has been observed in several cancer types. Several studies have found a correlation between increased SPOCK1 expression and cancer cell proliferation, invasion, metastasis and drug resistance.

According to The Cancer Genome Atlas (TCGA) SPOCK1 expression was significantly higher in cancer tissues compared to normal in cholangiocarcinoma, pancreatic adenocarcinoma, prostate adenocarcinoma, gastric adenocarcinoma, colon adenocarcinoma, head and neck squamous cell carcinoma, renal cell carcinoma, and squamous cell lung cancer. Higher SPOCK1 expression correlated with shorter overall survival in colon adenocarcinoma, head and neck squamous cell carcinoma, renal cell carcinoma, lung adenocarcinoma and uveal melanoma (75–77).

Increased SPOCK1 expression was also observed in human cirrhotic livers and in HCC, compared to normal controls. SPOCK1 was overexpressed in the tumor area compared to adjacent tissue and increased expression was associated with advanced clinical stage and metastasis (78,79).

CHD1L is the only known transcription factor of SPOCK1. It is a potent anti-apoptotic and pro-proliferative factor coded in the 1q21 region, that is frequently amplified in HCC. It activates transcription by binding to the promoter region of SPOCK1 (nt-1662 to +34). In human HCC samples, a positive correlation between SPOCK1 and CHD1L has been established. (78,80).

In the following section signaling pathways will be discussed in which SPOCK1 is involved. Downstream targets of SPOCK1 are members of matrix metalloproteinases (MMPs, MMP2, MMP9), proteins involved in the epithelial-mesenchymal transition (EMT), members of Wnt/β-catenin and phosphoinositide 3-kinase (PI3K)/ Protein kinase B (AKT) signaling pathways.

1.4.4.1. SPOCK1 in EMT

EMT plays a role in embryonic development and wound healing but also contributes to fibrosis and cancer progression. During this process, cells switch from immotile epithelial to a motile mesenchymal phenotype. TGF-β plays an important role in the induction of EMT and this switch in cell differentiation is driven by a set of transcription factors: Snail, Slug, Twist-related protein 1, zinc-finger E-box-binding homeobox 1 (ZEB1) and ZEB2 (81). Several studies have found that SPOCK1 is involved in EMT (82). The addition of TGF-β to the culture medium induced the expression of SPOCK1 in A549 non-small cell lung cancer (NSCLC) cell line (83). Similar findings has been observed in lung adenocarcinoma, breast cancer and pancreatic ductal adenocarcinoma cells (84–86). Alshargabi et al. found that SPOCK1 transgenic mice develop gingival hyperplasia and observed changes in markers of EMT, such as downregulation of E-cadherin and upregulation of vimentin in gingival tissue (87). Concomitantly, TGF-β, connective tissue growth factor (CTGF), Slug, a repressor of E-cadherin, was significantly upregulated. It was also found that TGF-β stimulation induced SPOCK1 expression in gingival keratinocytes but not in gingival fibroblasts (87).

Silencing of SPOCK1 in xenografts of the PC-3M prostate cancer cell line decreased the expression of Snail and Slug (88). Silencing of SPOCK1 in pancreatic cancer cell lines increased the expression of E-cadherin, and decreased the expression of vimentin and the EMT transcription factors (Snail, Slug, ZEB1 and ZEB2) (75). SPOCK1 overexpression induced Snail and Slug expression in the Caki-1 clear cell renal carcinoma cell line (89).

1.4.4.2. Participation of SPOCK1 in ECM remodeling

Degradation of the ECM is a key event in the process of tumor cell invasion, intravasation and extravasation. In SPOCK1 transgenic mice staining for type IV collagen revealed altered integrity of the gingival basement membrane. Higher levels of active-MMP2 and active-MMP9 were observed, with no change in the levels of the inactive form (87). Similar effects were observed in the QGY-7703 HCC cell line, where SPOCK1 overexpression promoted the expression and activation of MMP9. MMP9 inhibitor could reverse the effect of SPOCK1 overexpression on invasion (78). Transfection of an MMP2 expressing plasmid into the Caki-1 clear cell renal carcinoma cell line reversed the effects of SPOCK1 silencing on invasion. String analysis revealed that MMP14 and MMP16 were two of the top ten interactors of SPOCK1, both of which contribute to the activation of MMP2 and MMP9 (89). Berger et al. found that silencing SPOCK1 in BALB/c mice worsened the outcome of bacterial keratitis following P. aeruginosa-induced ocular infection. As a mechanism they identified lower MMP2 mRNA and protein levels in the SPOCK1 silenced mice, which is indispensable for wound healing and repair (90).

1.4.4.3. Wnt/ β-catenin signaling pathway

Knockdown of SPOCK1 in U87 MG glioma cell line significantly suppressed the expression of the Wnt and its downstream targets c-Myc and cyclin D1. This resulted in an increased cell fraction in G1 phase (91). Similar findings were observed in NSCLC cell lines, where SPOCK1 silencing decreased the levels of β-catenin, c-Myc and cyclin D1 together with decreased proliferation, migration and invasion rates (92).

1.4.4.4. PI3K/AKT signaling pathway

In-vitro SPOCK1 overexpression promoted proliferation and foci formation in QGY-7703 and PLC-8024 HCC cell lines trough Akt (78). Knockdown of SPOCK1 in the U87MG glioma cell line significantly downregulated the p-PI3K and p-Akt levels (91). Similar findings were observed in HCT116 colorectal cancer cells (93). Recombinant SPOCK1 protein activated the Akt signaling pathway in clear cell renal carcinoma cells (89). Platelet-derived growth factor (PDGF)-BB significantly increased SPOCK1 expression in the Lx2 cell line and in isolated rat hepatic stellate cells, which could be reversed by the PI3K inhibitor LY294002. In these cells, Three putative binding sites for FoxM1 were identified in the promoter region of SPOCK1. This suggests an upregulation

of SPOCK1 expression through the PI3K/Akt/FoxM1 pathway (79). SPOCK1 overexpression or recombinant SPOCK1 promoted Akt phosphorylation and consequently the expression of Cyclin B1, cyclin D1, MMP2, and MMP9. Furthermore, in rats, hepatic stellate cell-specific SPOCK1 knockdown ameliorated the thioacetamide-induced liver fibrosis (79).

1.4.4.5. Interaction of SPOCK1 with integrin α5β1

Immunoprecipitation of Lx2 lysate with anti-SPOCK1 antibody revealed that SPOCK1 interacts with integrin α5 and β1, suggesting a role as a SPOCK1 receptor. Blocking the integrin α5 and β1 receptors reversed the effects of recombinant SPOCK1 on proliferation and migration and on the expression of MMP2, MMP9 and on the phosphorylation of Akt in Lx2 cell line (79).

2. Objectives

Based on previous studies showing that overexpression of SPOCK1 is associated with poor prognosis in various cancer types, our hypothesis was that SPOCK1 is actively involved in the development and progression of the HCC. To address this hypothesis, first we aimed to evaluate the localization and physiological function of SPOCK1 in the liver. Second, we studied the role of SPOCK1 in carcinogenesis and progression of HCC, deciphering the underlying signaling pathways, and evaluated its potential as a diagnostic marker.

The specific objectives of our study were:

- To investigate the cellular localization and expression of SPOCK1 in normal human, mouse and rat livers.
- To study the SPOCK1 expression in human liver regeneration massive hepatic necrosis.
- To evaluate the SPOCK1 expression in cirrhotic human livers of various etiology, in HCC and in mouse DEN hepatocarcinogenesis model.
- To analyze the serum concentration of SPOCK1 in HCC patients.
- To develop SPOCK1 knock-in and knock-down in vitro models to perform functional assays and analyze the changes in signaling pathways.

3. Methods

3.1. Cell Cultures

HepG2 (ATCC HB-8065, purchased from American Type Culture Collection), HLE, Huh7 (JCRB0404, JCRB0403 respectively, purchased from Japanese Collection of Research Bioresources Cell Bank) HCC cell lines were maintained in Dulbecco's Modified Eagle Medium (DMEM) Low Glucose (D5546, Merck KGaA), supplemented with 10% fetal bovine serum (FBS; FB-1001B/500, Biosera), 2 mM L-glutamine (XC-T1715/100; Biosera), 100 units/ml penicillin, and 100 µg/ml streptomycin (P0781-100ML, Merck KGaA) (94).

3.2. SPOCK1 Silencing in HLE and Huh7 Cell Lines

SPOCK1 silencing in HLE and Huh7 cell lines was carried out using Lipofectamine™3000 (L3000008, Life Technologies, Carlsbad, CA, USA) and ON-TARGETplus Human SPOCK1 small interfering ribonucleic acid (siRNA, L013724-01-0005, Dharmacon Inc., Lafayette, CO, USA). We used the following target sequences to construct the siRNA: "CCUACAAAGAACAUCGUAA", "GGGUUGGACCUUCGAAUUU", "CGAUGGAGCCACAUUAAUA", and "GGUGUAAUGAGGAGGGCUA". Cells were seeded in 6-well plates at a density of 1.5 × 105 cell/well, 1 × 105 cell/well in case of Huh7 and HLE respectively and cultured for 24 hours before transfection. According to the manufacturer's instructions 6 µl of transfection reagent and 50 pmol of SPOCK1 siRNA or scrambled siRNA was used in 2000 µl of growth medium. Glyceraldehyde 3-phosphate dehydrogenase (GAPDH) siRNA was used to evaluate the transfection efficacy. Cells were harvested 48 hours post-transfection for further analysis (94).

3.3. SPOCK1 Expression Plasmids and Transfection of HepG2 Cells

Wild-type SPOCK1 expression plasmid was generated through polymerase chain reaction (PCR) cloning. The full-length open reading frame (ORF) of human SPOCK1 was amplified in two steps using Phusion High-Fidelity polymerase. Initially, outer primers (Forward (F)-out: 5′ GGCGGCGTGTGGCAGGAG 3′ and Reverse (R)-out: 3′ TAGAGAGCAACAATGGAGAAGAGACC 5′) were used for 30 cycles, utilizing cDNA derived from HLE cells as a template. In the subsequent PCR, inner primers (ORF-F: 5′

TTTTTGGATCCGAAATGCCTGCTATCGCGGTG 3′ and ORF-R: 3′ TTTTTC TCGAGCTACCATATGTACCCGACCTCATC 5′) were used, the product of the initial PCR serving as the template. The gel-purified fragment from the second PCR was inserted into a pcDNA™4/TO mammalian expression plasmid (V102020 Life Technologies, Carlsbad, CA, USA) through BamHI and XhoI restriction sites. Transfection was performed using the 100 µl tip of Neon Transfection System (MPK5000, Life Technologies) with 2 × 10^5 cells and 5 µg of either SPOCK1 pcDNA™4/TO or empty vector pcDNA™4/TO with the following parameters: 1,200 V, 50 ms, and 1 pulse. The cells were then seeded in 6-well plates with DMEM containing 20% FBS and 2 mM L-glutamine. Stable transfectants were selected in a growth medium supplemented with 500 µg/ml of Zeocin. Individual colonies were expanded, and the one with the highest SPOCK1 expression was selected and cultured for further experiments (94).

3.4. Bromodeoxyuridine (BrdU) Assay

SPOCK1 silencing or overexpression was performed as described above. The cells were cultured on coverslips in 6-well plate in complete growth medium for forty-eight hours after transfection. BrdU (B5002, Merck KGaA) was added to the culture medium in a concentration of 10 µM and incubated for 30 min at 37°C. The cells were fixed in methanol on -20°C for 10 min and washed. For DNA denaturation 2N HCl was used for 10 min at room temperature. The samples were washed and incubated with Anti-BrdU antibody for 1 h at room temperature. The slides were incubated with Alexa Fluor 488 secondary antibody and 4′,6-diamidino-2-phenylindole (DAPI, 1:200, D9542, 20 mg/ml stock concentration) (see antibodies used in Table 1). The stained slides were scanned with 3DHistech Pannoramic Confocal scanner and analyzed using CaseViewer CellQuant 2.2 (3DHISTECH Ltd., Budapest, Hungary) (94).

Table 1. Antibodies used

Primary Antibody	Host Species, Isotype	Manufacturer, Location	Catalog No.	Dilution (IHC, ICC, Blot, WES)
Anti-BrdU	Mouse, monoclonal (clone B44)	Becton, Dickinson and Company (BD),	347580	1:50 (ICC)

		Franklin Lakes, NJ, USA		
CDK4	Mouse, monoclonal (clone DCS-31 + DCS-35)	Thermo Fisher Scientific, Fremont, CA, USA	MS616P0	1:1000 (Western Blot)
CHD1L	Rabbit, polyclonal	Merck KGaA, Darmstadt, Germany	HPA028670	1:1000 (IHC)
Cleaved Caspase-3	Rabbit, monoclonal (clone 5A1E)	Cell Signaling Technology, Danvers, MA, USA	9664	1:1000 (Western Blot)
Cross-Adsorbed Secondary Antibody, Alexa Fluor 568	Goat anti-Rabbit IgG	Invitrogen, CA, USA	A11011	1:200
GAPDH	Rabbit, monoclonal (clone 14C10)	Cell Signaling Technology, Danvers, MA, USA	2118	1:50 (WES)
Highly Cross-Adsorbed Secondary Antibody, Alexa Fluor 488	Goat anti-Mouse IgG	Invitrogen, CA, USA	A11029	1:200 (ICC)
Highly Cross-Adsorbed Secondary Antibody, Alexa Fluor 488	Donkey anti-Rabbit IgG	Invitrogen, CA, USA	A21206	1:200 (ICC)
p21	Rabbit, monoclonal (clone EPR18021)	Abcam, Cambridge, UK	ab188224	1:1000 (Western Blot)
p27	Rabbit, polyclonal	Abcam, Cambridge, UK	ab64949	1:1000 (Western Blot)
p53	Rabbit, monoclonal (clone EP155Y)	Abcam, Cambridge, UK	ab33889	1:1000 (Western Blot)

pAKT (T308)	Rabbit, monoclonal (clone C31E5E)	Cell Signaling Technology, Danvers, MA, USA	2965	1:1000 (Western Blot)
SPOCK1	Rabbit, polyclonal	Merck KGaA, Darmstadt, Germany	HPA07450	1:100 (IHC), 1:200 (ICC), 1:1000 (Western Blot), 1:50 (WES)
Syndecan-1	Mouse monoclonal IgG, clone MI15	Dako	M7228	1:100 (IF)
β-Actin	Mouse, monoclonal (clone AC-74)	Merck KGaA, Darmstadt, Germany	A2228	1:2000 (Western Blot)
β-Catenin	Rabbit, polyclonal	Cell Signaling Technology, Danvers, MA, USA	9562	1:1000 (Western Blot)
Vimentin	Mouse, monoclonal (clone V9)	Agilent DAKO	M0725	1:200 (IF)

3.5. Primary rat hepatocyte isolation

Fisher F344 rats were purchased from Charles River Laboratories (É cully, France) and housed in plastic cages (556 × 334 mm, AnimaLab, Poznań , Poland) under standard conditions: 12 h of light–dark cycles, constant temperature (23°C), and humidity (22%). Standard rodent chow (V1535000, SSNIFF, Soest, Germany; 15-mm pellets) was provided ad libitum. Hepatocyte isolation was performed using a two-step collagenase perfusion method. The animals were anesthetized and the abdomen was opened with a midline incision through the linea alba. The intestines were moved to the right side to access the portal vein. This was canulated and an incision was made on the vena cava inferior. The liver was perfused with pre-warmed (37°C) Leffert's buffer (10 mM HEPES, 3mM KCl, 130 mM NaCl, 1 mM NaH2PO4, 10 mM D-glucose, pH7.4) containing 0.5 mM EGTA for 5 minutes followed by perfusion with Leffert's buffer for 2 minutes. Collagenase (C5138, Merck KGaA, 0.33 mg/ml) was dissolved in Leffert's buffer containing 5 mM CaCl2.2H2O. The livers were dissociated in cold Leffert's buffer containing 5 mM CaCl2.2H2O. The cells were filtered through a 100-µm nylon filter, and then the suspension was centrifuged for 5 min at 50g to separate hepatocytes from non-

parenchymal cells. The pellet was resuspended and centrifuged three times in total. The hepatocytes were co-cultured with Lx2 hepatic stellate cell line (a kind gift from Dr. Scott Friedman) on coverslips in 2 to 1 ratio in Williams' Medium E (W4128, Merck KGaA) supplemented with 1x Insulin-Transferrin-Selenium (41400045, Life Technologies), 2mM L-glutamine and 4% FBS. After 24h the cells were washed with phosphate-buffered saline (PBS) and fixed with ice cold methanol for 10 minutes. The cells were washed and were incubated with the primary antibodies overnight at 4°C. The coverslips were washed and were incubated for 1h at room temperature with Alexa Fluor 488- and Alexa Fluor 568-conjugated secondary antibodies and DAPI (1:200, D9542, 20 mg/ml stock concentration). The samples were mounted using Fluoromount (F4680; Merck KGaA) (94).

3.6. Diethyl-nitrosamine Induced Hepatocarcinogenesis

Animal experiments were approved by the Ethics Committee of the Animal Health Care and Control Institute, Csongrád County, Hungary (protocol code XVI/03047-2/2008) and conducted as described previously (44). DEN hepatocarcinogenesis model was carried out by a single intraperitoneal dose of DEN in 15 days old C57/Black mice at 15 μg/ g body weight. 26 DEN-treated wild-type C57/Black mice and 16 untreated C57/Black controls were studied and sacrificed at 9-months post-exposure. The liver samples were formalin-fixed paraffin-embedded (FFPE) and used for immunohistochemistry (94).

3.7. Human Samples

Surgical liver specimens were obtained and handled following the guidelines of the Semmelweis University Regional and Institutional Committee of Science and Research Ethics (TUKEB, permit number: 155/2012) and the Medical Research Council Committee of Science and Research Ethics (permit number: 61303-2/2018/EKU).

Human serum samples were collected from patients with HCC and from those without HCC diagnosis and handled following the guidelines of the Semmelweis University Regional and Institutional Committee of Science and Research Ethics (TUKEB, permit number: IV/2734-3/2022/EKU) and the Medical Research Council Committee of Science and Research Ethics (permit number: BM/12102- 3 /2023/EKU) (94).

3.8. Immunohistochemistry (IHC)

FFPE human and mouse liver sections were deparaffinized and rehydrated. BOND Epitope Retrieval Solution 1 (AR9961, Leica Biosystems, Newcastle, UK) was used for heat induced antigen retrieval in a pressure cocker for 20 minutes. Endogenous peroxidase was blocked for 20 minutes at room temperature using 10% H2O2 in methanol. The sections were then rinsed with PBS with Tween-20 (0.05% Tween-20) followed by a 10-minute incubation with Novocastra Protein Block (RE71102, Leica Biosystems) at room temperature. The sections were incubated with the primary antibody overnight at 4°C (see antibodies used in Table 1). The following day, the sections were washed for 1 hour and incubated with HISTO-Labeling System (30011.R500, Department of Immunology and Biotechnology, Pécs, Hungary) for 30 minutes at room temperature. The staining was visualized using diaminobenzidine at a 1:50 dilution (ImmPACT DAB, SK4105, Vector Laboratories, Burlingame, CA, USA), followed by counterstaining with hematoxylin. Finally, the sections were dehydrated and mounted using BIOMOUNT (BMT-500, BIOGNOST D.O.O, Zagreb, Croatia). The stained slides were scanned at ×20 magnification using a Panoramic P1000 scanner, and quantitative analysis was conducted with CaseViewer DensitoQuant 2.2 (3DHISTECH Ltd., Budapest, Hungary) (94).

3.9. Double-Fluorescent Immunocytochemistry

The deparaffination, rehydration and the antigen retrieval of the FFPE human liver sections was performed as described above. The Novocastra Protein Block was applied for 10 minutes and the SPOCK1 and syndecan-1 primary antibodies were incubated overnight at 4°C (see antibodies used in Table 1). The sections were washed with PBS and incubated with anti-rabbit Alexa Fluor 568, anti-mouse Alexa Fluor 488 and DAPI (1:200, D9542) for 1 hour on room temperature. The slides were washed and mounted using Fluoromount (F4680; Merck KGaA) (94).

3.10. Mitochondria labeling and fluorescent immunocytochemistry

Huh7 cells were seeded on coverslips in 6-well plates at a density of 2×10^5 cells per well and cultivated in complete growth medium for 24 hours. For labeling the mitochondria fresh medium was added containing 200nM MitoTracker® Red CMXRos (M46752, Life Technologies, Carlsbad, CA, USA) and cultured for 30 minutes. The cells were washed

in prewarmed PBS and fixed with methanol for 10 minutes on -20°C than washed with PBS. The samples were incubated with SPOCK1 primary antibody overnight on 4°C. The following day, the samples were washed three times with PBS and incubated with Alexa Fluor 488-conjugated anti rabbit secondary (see antibodies used in Table 1) antibody for 1 hour at room temperature. Negative controls were prepared by omitting the primary antibodies. The slides were then mounted using Fluoromount (F4680; Merck KGaA) and were analyzed by laser scanning confocal microscopy (MRC 1024; Bio-Rad, Hercules, CA, USA) (94).

3.11. Human Phospho-Kinase Array

Relative site-specific phosphorylation of 43 kinases was determined using Human Phospho-Kinase Array (ARY003B, R&D Systems, Minneapolis, MN, USA). According to the manufacturer's instructions, protein lysates of SPOCK1-silenced and control samples were incubated with the membranes, 400 μg of protein was used on each array. The signal was detected with iBright FL1000 Imaging Systems and analyzed with Carpentier G. Protein Array Analyze for ImageJ (2010) available online: http://rsb.info.nih.gov/ij/macros/toolsets/ Protein Array Analyzer.txt (94).

3.12. Automated Western Blotting System (WES™)

WES™ (ProteinSimple, San Jose, CA, USA, a Bio-Techne Brand) automated capillary-based electrophoresis instrument was used to analyze the relative changes in target proteins according to the manufacturer's instructions. The cells were harvested at 70%–80% confluency in lysis buffer containing 20 mM Tris, 150 mM NaCl, 2 mM EDTA (pH 8), and 0.5% Triton X-100 supplemented with protease and phosphatase inhibitors (P8340, Merck KGaA). After sonication and centrifugation, the supernatant was stored on -80°C for further analysis. Conditioned media were collected and concentrated using 10,000 NMWL centrifugal filters (Amicon Ultra-4, UFC801024, Merck Millipore, Burlington, MA, USA). Protein Assay Dye Reagent Concentrate (500-0006, Bio-Rad, CA, USA) was used to measure the protein concentration. The protein samples were diluted to a concentration of 1 μg/μl in 0.1× Sample Buffer (ProteinSimple, 042-195) and Fluorescent Master Mix was added in a 1:4 ratio and incubated for 5 minutes at 95°C. Equal amount of protein sample, the primary and secondary antibodies (see antibodies used in Table 1), and all the reagents were loaded onto the plate according to the

manufacturer's instruction. The electrophoresis was performed using the 12230 kDa of Separation Module (SM-W004, ProteinSimple) with the following settings: separation (395V, 30 min), blocking (5 min), incubation with primary antibody (30 min), incubation with secondary antibody (30 min), and chemiluminescent detection (15 min). The images were analyzed using Compass software (San Jose, CA, USA) (94).

3.13. Enzyme-linked immunosorbent assay (ELISA)

Human SPOCK1 Sandwich ELISA Kit (LS-F25604, Vector Laboratories, Inc., Newark, CA, United States) was performed according to the manufacturer's instructions. Briefly, 100µl per well of blank, standard and serum sample was added and incubated 1 hour at 37°C. The liquids were aspirated from each well and 100µl "Detection Reagent A" working solution was added and incubated 1 hour at 37°C. The liquids were aspirated, and the wells were washed three times. 100µl "Detection Reagent B" was added and incubated 30 minutes at 37°C. The liquids were aspirated, and the wells were washed five times. 90µl of TMB Substrate solution was added to each well and incubated 15 minutes than 50µl of Stop Solution was added. The optical density value was determined at 450 nm using Labsystems Multiskan MS 352 microplate reader (94).

3.14. Quantitative reverse transcription PCR (RT-qPCR)

Total RNA was extracted using the RNeasy Plus Mini Kit (74134, Qiagen, Germany). 1 µg RNA was used for reverse transcription with High-Capacity cDNA Reverse Transcription Kit (4368814, Life Technologies) following the manufacturer's instructions. TaqMan Fast Advanced Master Mix (4444556, Life Technologies) was used to determine the expression level of SPOCK1 (TaqMan Gene Expression Assay, assay ID: Hs00270274_m1; Life Technologies) with the following protocol: UNG incubation at 50°C for 2 minutes, polymerase activation at 95°C for 2 minutes, followed by 40 cycles of denaturation at 95°C for 1 second, and annealing and elongation at 60°C for 20 seconds. β-actin (4326315E, Life Technologies) was used as endogenous control to normalize the relative expression level (94).

3.15. Statistical Analysis

Statistical analysis was performed with GraphPad Prism Version 10.3.1 (GraphPad Software, La Jolla, CA, USA), using two-tailed unpaired t-tests, one-way ANOVA with

Dunnett's multiple-comparison tests and Mann Whitney U test. Significance was defined as *p < 0.05, **p < 0.01, and ***p < 0.001. The correlation between the SPOCK1 expression and survival was assessed using KM plotter (https://kmplot.com/analysis/) and compared with the log rank test and the hazard ratios and the 95% confidence intervals were estimated by Cox proportional hazards model (94).

4. Results

4.1. SPOCK1 expression in normal human liver

We evaluated the baseline SPOCK1 expression in normal human livers. For this purpose, we used normal area from peritumoral tissues where the normal lobular structure of the liver was preserved (Figure 2A, 2C). Hepatocytes adjacent to both central and portal vein exhibited intense granular SPOCK1 expression (Figure 2B, 2D). The smooth-muscle cells in the arterial wall showed intense positive reaction as well, thus we used this as internal positive control (Figure 2E, 2F).

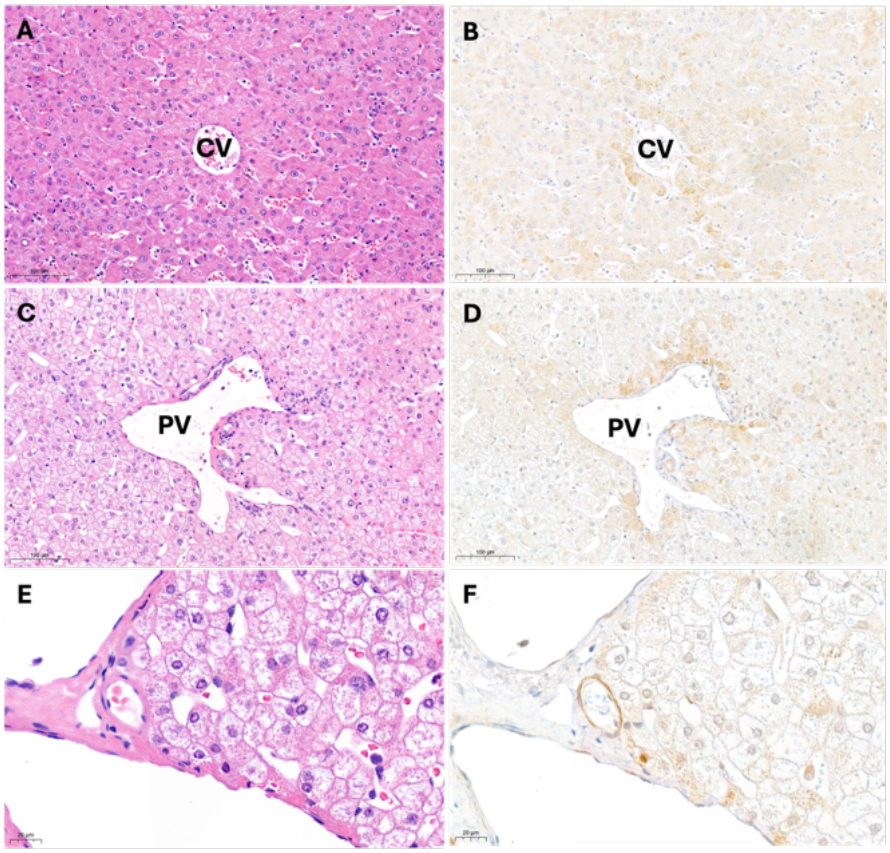

Figure 2. Expression of SPOCK1 in normal liver. The normal, lobular structure of the liver was preserved (A, C). Intense, granular staining pattern was seen in hepatocytes around the central vein (CV) and the portal vein (PV) on SPOCK1 IHC (B, D). Arterial wall at higher magnification (E), which showed intense positivity on SPOCK1 IHC (F), and we used as an internal positive control. Scale bar A-D 100 μm; E-F 20 μm.

4.2. SPOCK1 expression of isolated rat hepatocytes

We isolated primary rat hepatocytes and co-cultured with Lx2 human hepatic stellate cell line to evaluate the SPOCK1 expression in these two cell types. We performed SPOCK1 fluorescent immunocytochemistry and we used vimentin as a fibroblast marker. High SPOCK1 expression and a granular staining pattern was observed in the hepatocytes, however no SPOCK1 expression was detected in the hepatic stellate cell line (Figure 3).

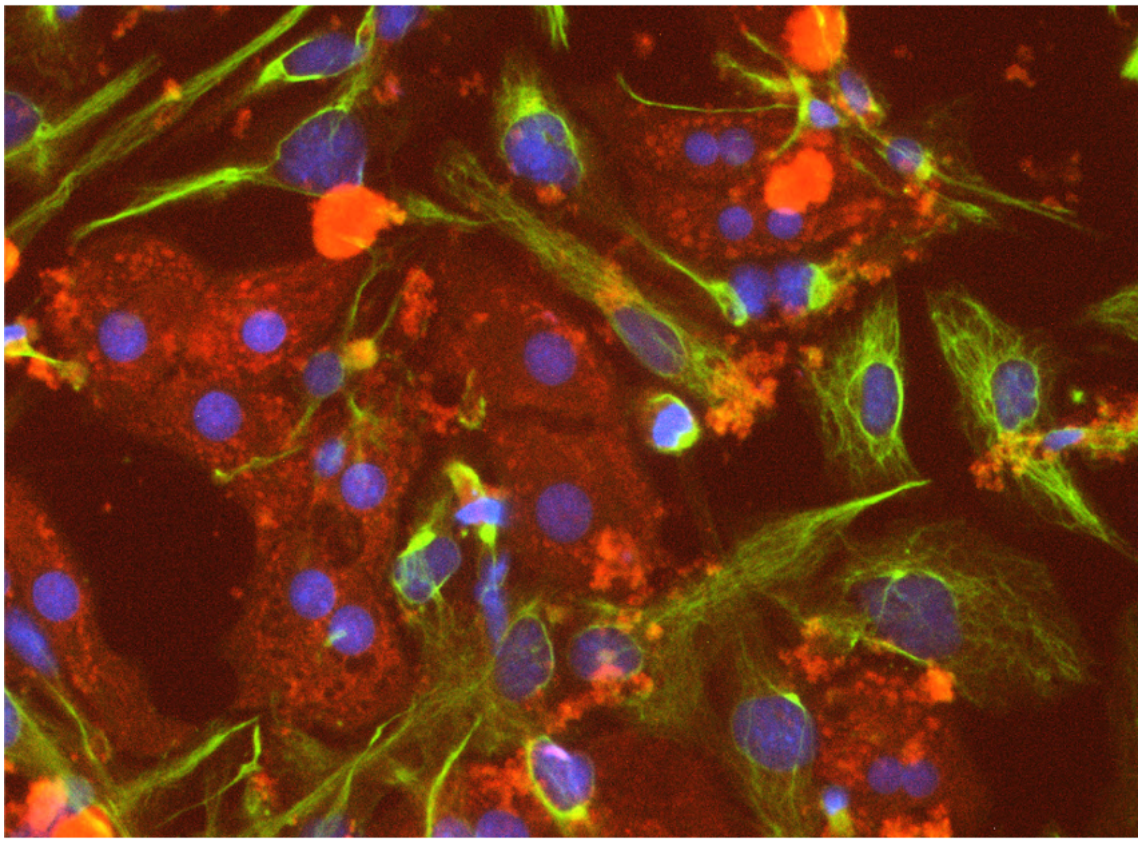

Figure 3. SPOCK1 expression in a co-culture model comprising primary rat hepatocytes and the Lx2 hepatic stellate cell line. Hepatocytes expressed high level of SPOCK1 (red) and it showed granular cytoplasmic staining pattern. Lx2 cells identified by vimentin positivity (green) showed no SPOCK1 expression. Blue – DAPI (95).

4.3. Subcellular localization of SPOCK1

The granular staining pattern suggest that the intracellular localization of the SPOCK1 is related to a cellular organelle. To verify this, we labeled the mitochondria using MitoTracker® Red CMXRos in Huh7 human cells line (Figure 4B) and carried out SPOCK1 fluorescent immunostaining (Figure 4A) on these samples. We observed the co-

localization of the two markers (Figure 4C), suggesting that the SPOCK1 is localized to the mitochondria.

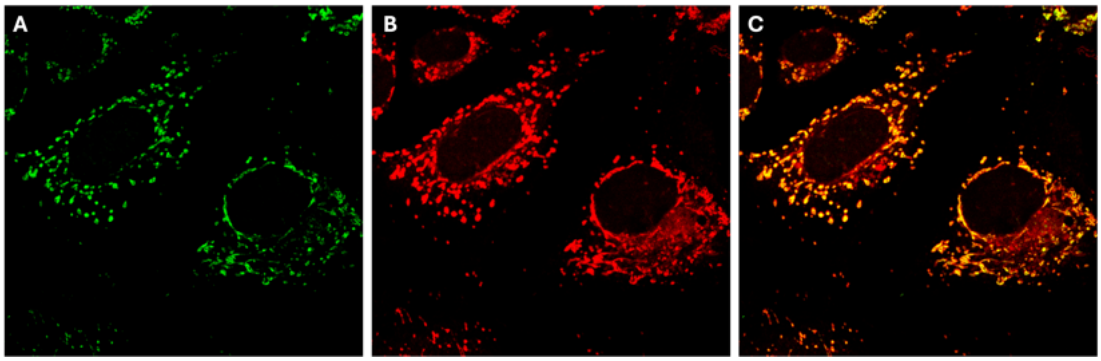

Figure 4. Co-localisation of SPOCK1 (green) and MitoTracker® (red) mitochondrial marker is shown. Representative images display SPOCK1 fluorescent immunostaining (A) and MitoTracker® Red CMXRos mitochondrial marker (B) in Huh7 cells. The merged image (C) shows co-localisation (appearing yellow), suggesting that SPOCK1 localizes to mitochondria. Images were taken at 100x magnification.

4.4. SPOCK1 expression during human liver regeneration

We assessed the SPOCK1 expression during the controlled hepatocyte proliferation in regenerating human livers. We collected FFPE human liver samples from our archive, explanted due to acute liver failure caused by massive hepatic necrosis, and grouped them based on the histologic pattern (10): 1) regeneration from dedifferentiated hepatocytes (n=5); 2) regeneration trough progenitor cells, forming regenerative foci (n=3). In the first group of regeneration, surviving hepatocytes dedifferentiate and they are organized into acinar structures containing bile in their lumens (Figure 5A, 5C). These hepatocytes showed intense, diffuse staining on SPOCK1 IHC without preferential periportal or pericentral localization (Figure 5B, 5D).

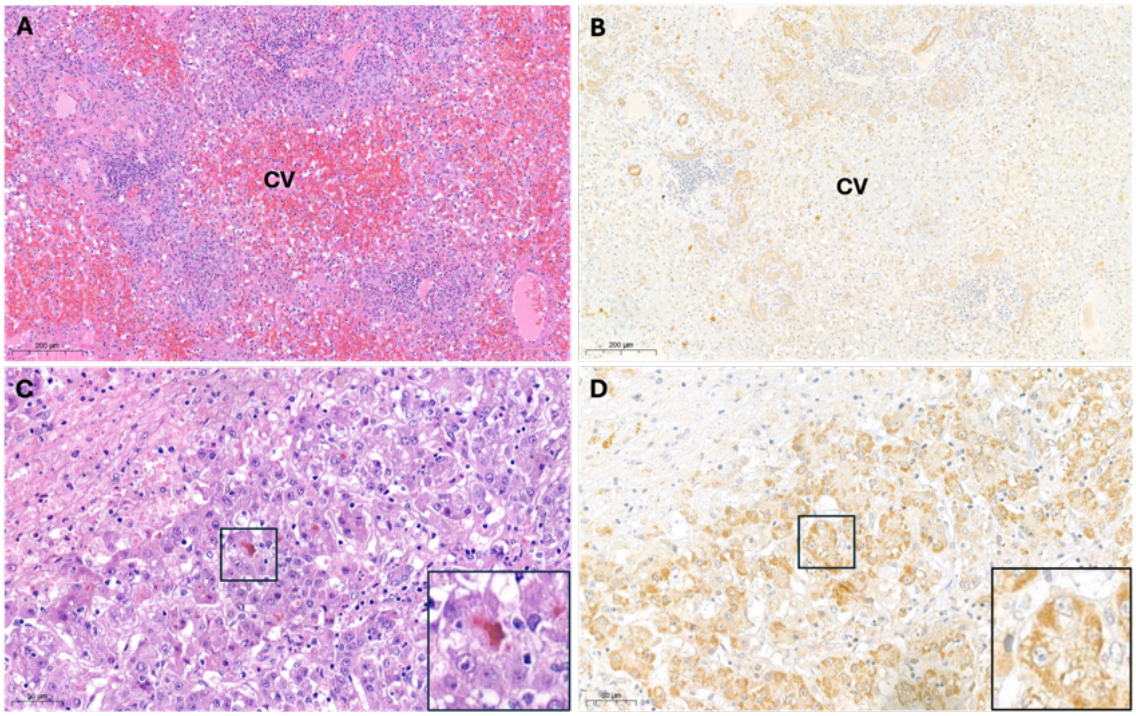

Figure 5. Hematoxylin and eosin (HE) and SPOCK1 IHC in the regeneration group from dedifferentiated hepatocytes. (A) HE staining of massive hepatic necrosis. (B) Low magnification image of SPOCK1 IHC. (C) Higher magnification image showed surviving hepatocytes arranged in acinar structures (inset) which expressed high level of SPOCK1 (D). Scale bar (A)(B) 200μm, (C)(D) 50μm

In the regeneration group from progenitor cells intense ductular reaction was observed in the periportal area. In the ductules, larger cells were seen with pale eosinophilic cytoplasm resembling hepatocyte morphology (Figure 6A, 6C). These cells showed increased SPOCK1 expression compared to the surrounding ductular cells (Figure 6D). Besides the intense positive reaction of the arterial wall used as an internal control, faint staining was observed in the regenerative foci (Figure 6B).

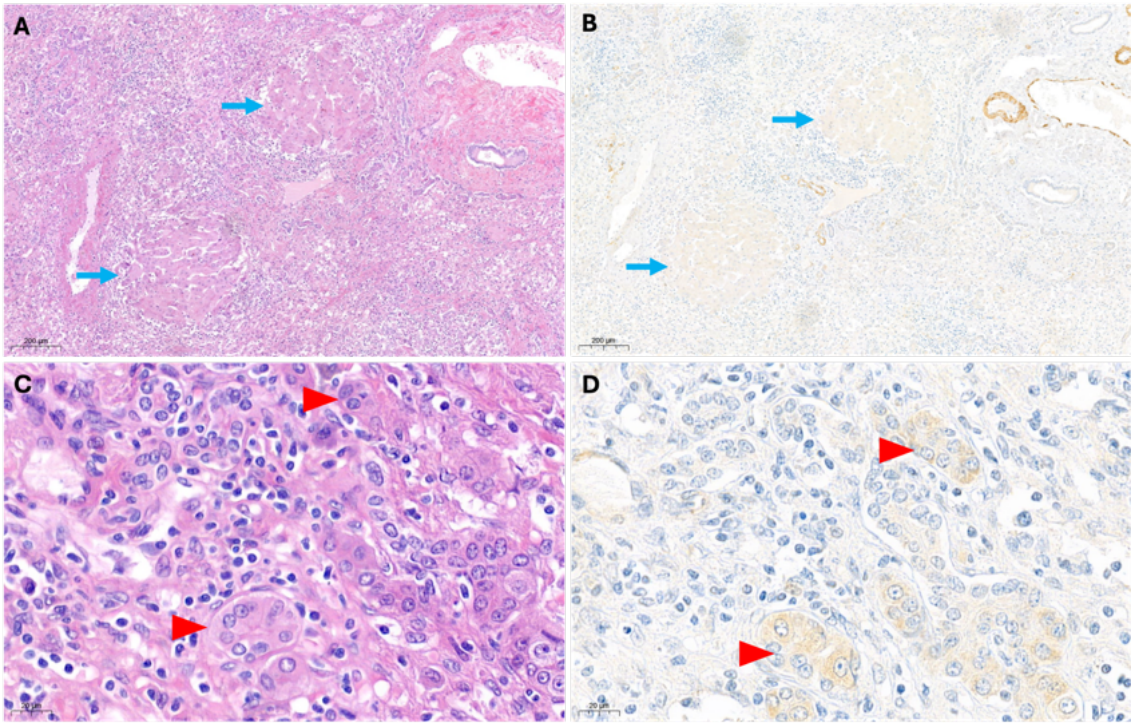

Figure 6. SPOCK1 IHC in regeneration group from progenitor cells. (A) HE staining of regenerative foci (blue arrow). (B) These showed low SPOCK1 expression on IHC. (C) Higher magnification image showed the ductular proliferation. (D) Larger cells in certain ductules (red arrowhead) resembling hepatocytes showed positivity on SPOCK1 IHC staining (D). Scale bar (A)(C) 200µm, (B)(D) 20µm

4.5. SPOCK1 expression in human liver cirrhosis and HCC

We collected 58 human liver samples and prepared tissue microarray from patients diagnosed with liver cirrhosis and HCC of various etiology, and hemangioma surrounding samples as control. To evaluate the SPOCK1 expression we performed IHC.

The normal control livers (Figure 7A) showed positive staining in hepatocytes surrounding the central and portal veins as described above. Increased expression of SPOCK1 was observed in the cirrhotic livers (Figure 7B) where the cirrhotic nodules showed intense granular staining pattern. Apart from the blood vessels, the connective tissue was mostly negative. Similar staining pattern was observed in HCC as well (Figure 7C).

We quantified the expression level of SPOCK1 by densitometry and calculated the H-scores (Figure 7D). This revealed significantly higher expression in HCV-associated

cirrhotic and HCC samples as well as in samples of unknown etiology when compared to control livers. Cirrhotic and HCC samples with alcoholic etiology showed elevated SPOCK1 expression, however this increase was not statistically significant. Cirrhotic and HCC samples of the same etiology showed similar expression level in all cases.

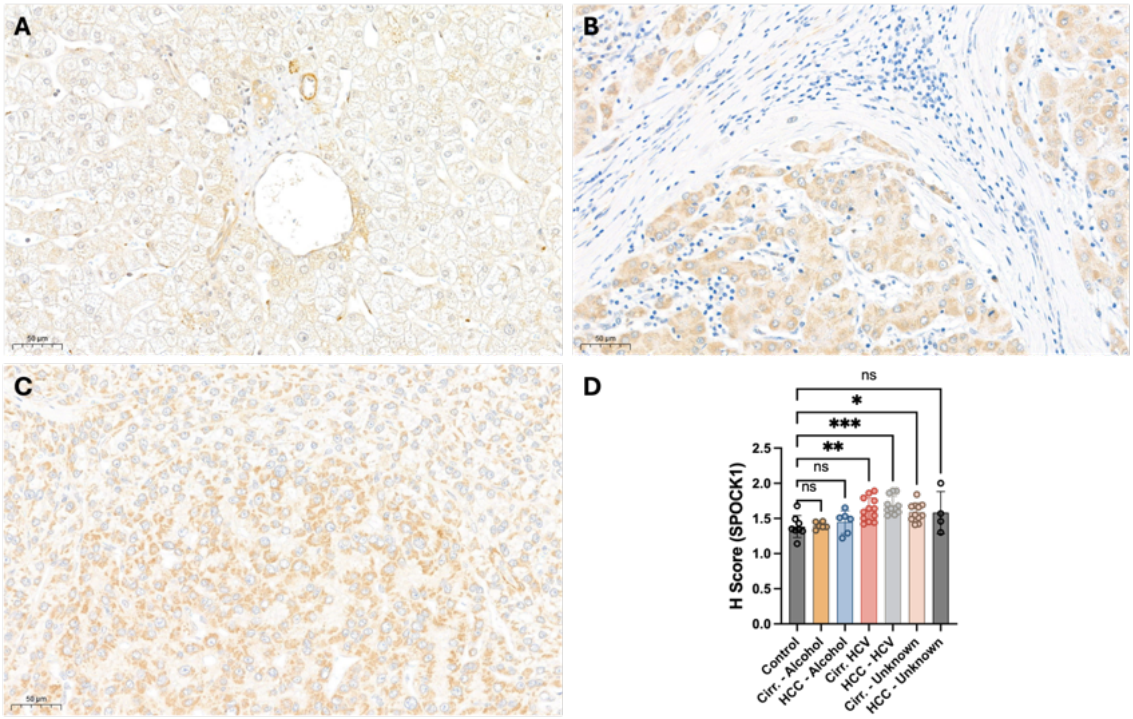

Figure 7. Representative images of SPOCK1 IHC on control, cirrhotic and HCC liver samples. (A) In control samples periportal hepatocytes showed intense positivity on SPOCK1 IHC. Increased expression was also observed in cirrhotic livers (B) and in HCC (C). Quantification of SPOCK1 expression by densitometry showed significant increase in case of HCV related cirrhosis and HCC also in case of cirrhosis of unknown etiology. Data is presented as mean ± SD, alcohol-related cirrhosis n=6; alcohol-related HCC n=6; HCV-related cirrhosis n=12; HCV-related HCC n=11; cirrhosis of unknown etiology n=11; HCC of unknown etiology n=4; control samples-hemangioma surrounding area n=8. Statistical analysis was performed using one-way ANOVA followed by Dunnett's multiple-comparison test (94).

We validated our results by performing RNA-seq based analysis using TNMplot publicly available tool (www.tnmplot.com) to compare the SPOCK1 expression in HCC and normal control samples or in HCC and paired surrounding liver tissues. This tool uses datasets collected from GEO, GTEx, TCGA, and TARGET databases. Statistical analysis revealed significant increase in SPOCK1 gene expression in HCC samples compared to

normal livers (Figure 8A). Moreover, the expression of SPOCK1 was also elevated in HCC samples compared to the surrounding normal area (Figure 8B). High SPOCK1 gene expression correlated with significantly shorter overall survival in HCC patients (hazard ratio 1.57 and 95% confidence interval 1.05-2.32) (Figure 8C) (96).

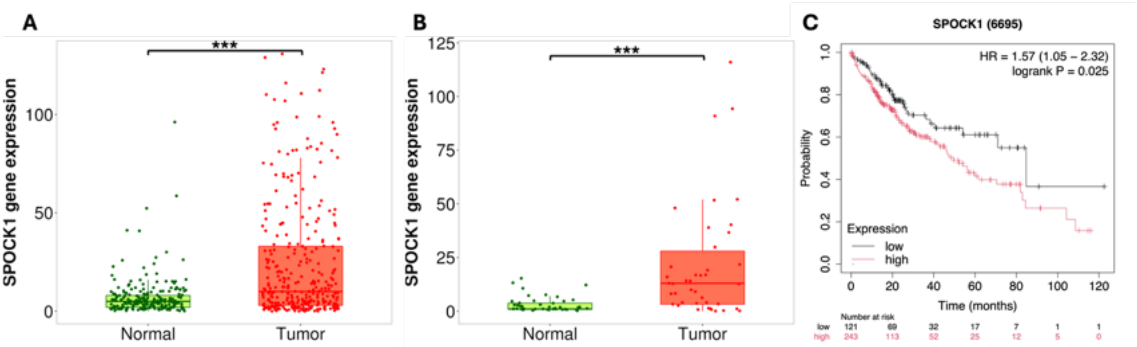

Figure 8. (A, B) Comparison of SPOCK1 gene expression in HCC and normal samples from TNMplot database. (A) SPOCK1 gene expression showed a significant increase in HCC patients (n=371), compared to liver samples of non-tumorous patients (N=225), (B) similar trends are observed when comparing paired tumor and adjacent normal tissues (n=50, n=50 respectively). (C) Kaplan-Meier plots showing overall survival of HCC patients. High SPOCK1 gene expression was associated with significantly shorter survival (the patients were divided by the lower tertile). (A)(B) Statistical analysis was performed using Mann Whitney U test, ***<0.001.

Syndecan-1 is the major proteoglycan of the liver, and our previous studies showed that overexpression of the human syndecan-1 protects against DEN induced hepatocarcinogenesis in mice. Thus, we aimed to compare the expression level of syndecan-1 and SPOCK1 in human liver cirrhosis and HCC. Syndecan-1 showed strong membranous staining pattern on hepatocytes in the cirrhotic nodules. The SPOCK1 was strongly expressed in the smooth muscle cells of the arterial wall, while faint positivity was observed in the hepatocytes (Figure 9A). The micro-metastases of HCC in the connective tissue showed high SPOCK1 expression whereas the expression of the syndecan-1 decreased (Figure 9B).

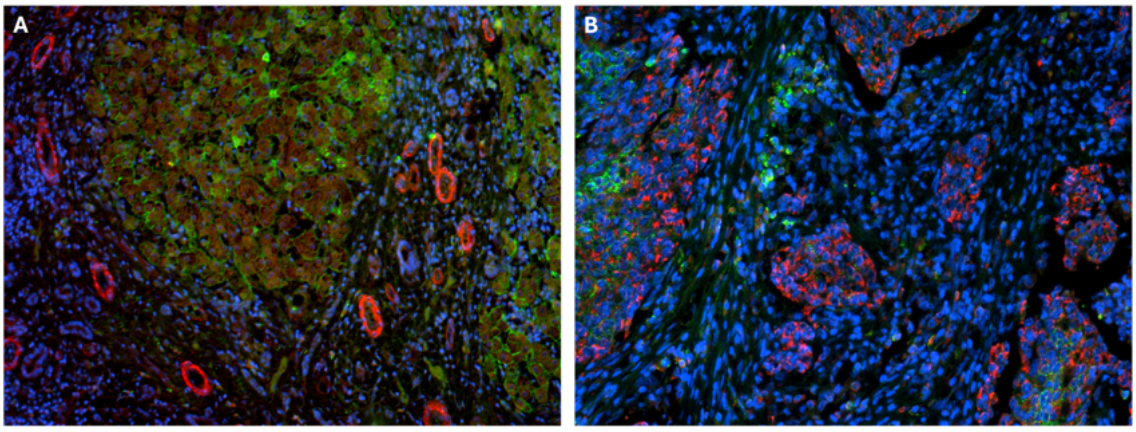

Figure 9. Expression of syndecan-1 and SPOCK1 in cirrhosis and in micro-metastases of the HCC. (A) Representative image of double fluorescent immunostaining in human cirrhotic liver. Intense membranous staining of syndecan-1 (green) was observed on the hepatocytes in the cirrhotic nodules, however these hepatocytes showed weak SPOCK1 positivity (red). The arterial wall showed intense positive reaction. (B) The micro-metastases in the connective tissue showed high SPOCK1 (red) expression whereas decreased syndecan-1 (green) expression was observed in these cells. DAPI – blue, (A) 10X, (B) 20X magnification (94).

4.6. SPOCK1 expression during DEN hepatocarcinogenesis in mice

We designed an experimental mouse model to analyze the alteration in SPOCK1 expression during the DEN hepatocarcinogenesis. This is a well described model where focal hepatic lesions are induced by 9 months. First basophilic foci appear on the HE staining, these are composed of altered hepatocytes (because of high cytoplasmic RNA content), with high nuclear to cytoplasmic ratio and crowded appearance. These lesions progress to trabecular hepatocellular carcinoma (97). The arterial wall, pericentral and periportal hepatocytes showed high expression of SPOCK1 in the control livers, similar staining pattern observed in normal human livers (Figure 10A). Increased SPOCK1 expression was detected 9 months after the DEN exposure in the foci (Figure 10B). Intense positive reaction of the CHD1L (Figure 10C), the known transcription factor of the SPOCK1 on these samples further strengthens our results.

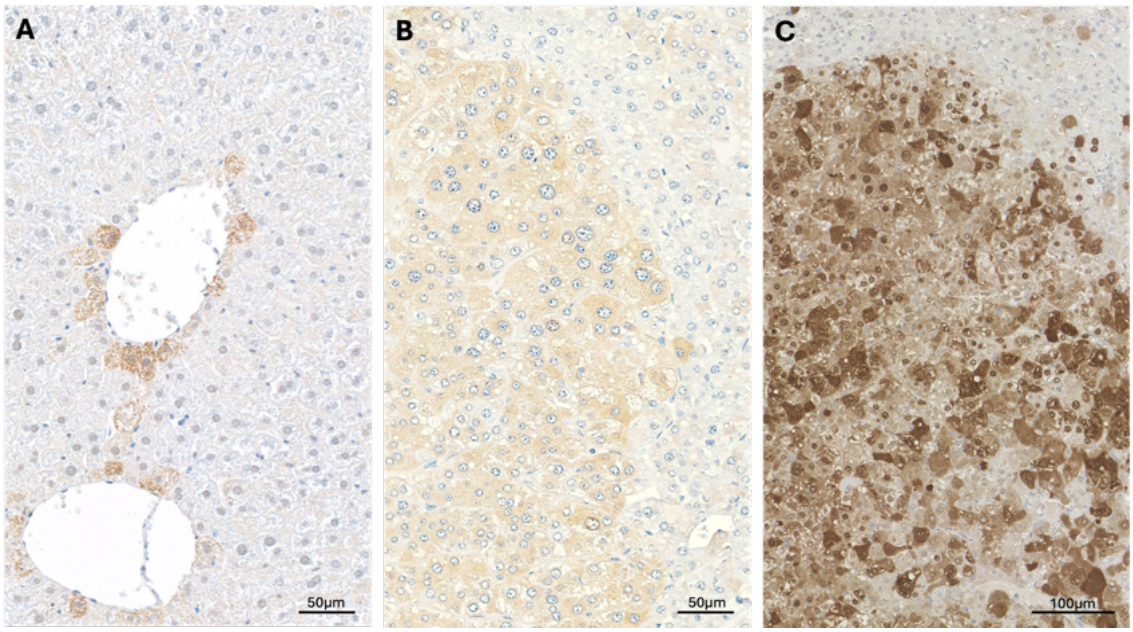

Figure 10. Expression of SPOCK1 in DEN hepatocarcinogenesis mouse model. (A) In control mouse livers SPOCK1 showed intense positive reaction on IHC in the pericentral hepatocytes. (B) Nine months after the DEN exposure SPOCK1 expression was detected in foci. (C) CHD1L IHC showed increased expression and nuclear localization at 9-month time point. Scale bar (A), (B) 50 µm, (C) 100 µm (94).

4.7. Detection of secreted SPOCK1 in human HCC cell lines and serum from HCC patients

SPOCK1 carries a signal sequence characteristic of extracellular proteins, and we investigated the localization of the SPOCK1 in cellular and extracellular compartments in vitro. HLE, Huh7 and HepG2 human HCC cell lines were cultured and SPOCK1 was detected by WES capillary electrophoresis in the cellular fraction and secreted in the conditioned medium (Figure 11A). Interestingly, protein electrophoresis showed strong bands of different molecular weight, suggesting a different glycosylation pattern of SPOCK1 in the three cell lines. In HLE and HepG2 the dominant form was around 66 kDa, while in Huh7 it was at 116 kDa.

Our results, showing that HCC cell lines secrete high levels of SPOCK1 in culture media prompted us to study its concentration in human serum samples. Serum samples were collected from patients with HCC and from those without HCC and analyzed by ELISA. In HCC patients the serum level of SPOCK1 increased 2.2 folds, however this change was not significant (Figure 11B).

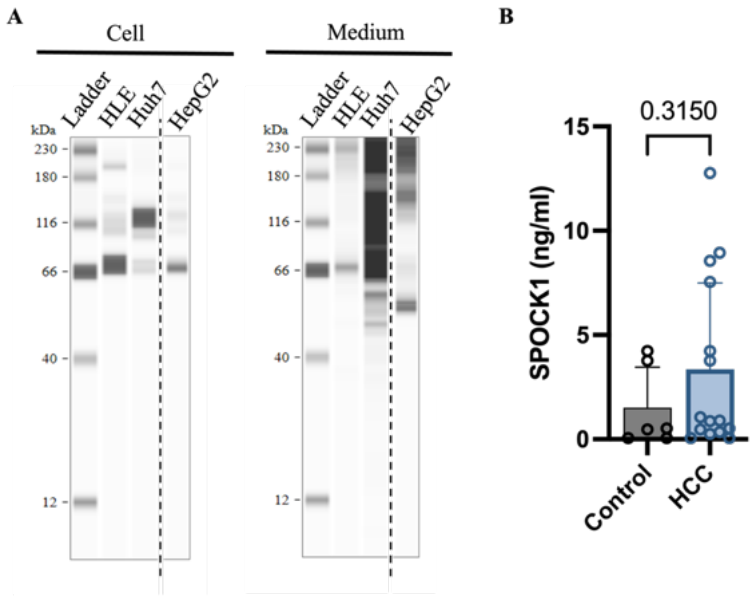

Figure 11. SPOCK1 detection in the culture medium of the HCC cell lines and in human serum samples. (A) SPOCK1 was present in the cells and also in the conditioned medium detected with capillary electrophoresis of the three HCC cell line. Dashed line: the microcapillary electrophoresis was performed separately. (B) ELISA revealed elevated levels of SPOCK1 in the serum of HCC patients compared to control patients without HCC. Data is presented as the mean ± SD, control group n=6, HCC group n=15. Statistical analysis was performed using unpaired t-test (94).

4.8. Effect of SPOCK1 on the proliferation of the human HCC cell lines

We used siRNA to silence SPOCK1 expression in human HLE and Huh7 HCC cell lines. The SPOCK1 mRNA expression decreased by 0.07- and 0.292-fold in HLE and Huh7 cell lines respectively, tested by RT-qPCR (Table 2). Interestingly, the intracellular level of SPOCK1 protein remained constant after silencing with siRNA, as measured by WES capillary electrophoresis. In contrast, secreted levels of SPOCK1 protein decreased in HLE and Huh7 cell lines (Figure 12).

Table 2. Downregulation of SPOCK1 mRNA measured by RT-qPCR after siRNA silencing in HLE and Huh7 cell lines

Cell line	Relative quantification (fold change)	95% CI
HLE	0.07	0.046-0.109
Huh7	0.292	0.139-0.613

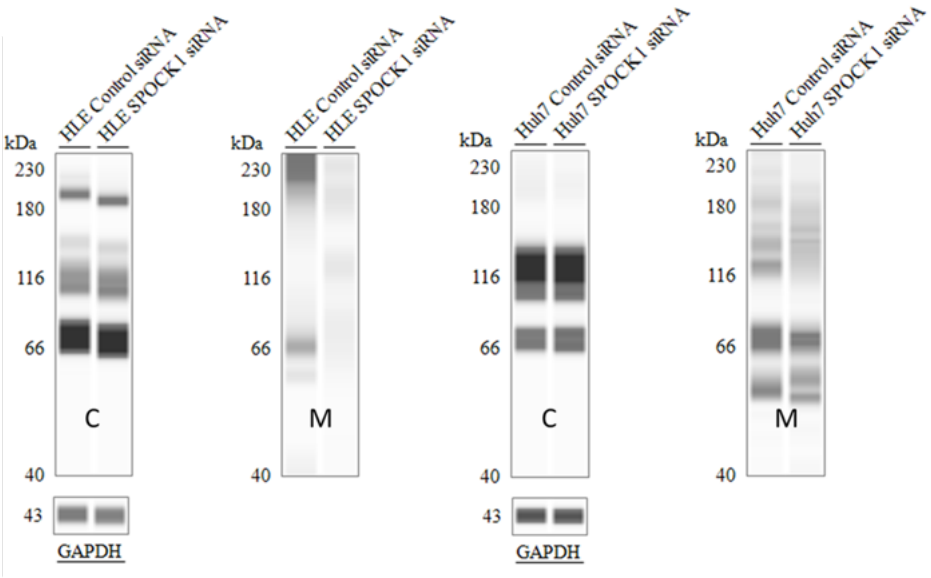

Figure 12. Silencing SPOCK1 in HLE and Huh7 cell lines decreased the level of secreted SPOCK1. Expression of SPOCK1 measured by WES capillary electrophoresis showed similar level of intracellular SPOCK1 ("C") after silencing using siRNA. Interestingly the secreted SPOCK1 was reduced in the conditioned medium ("M") (94).

To study the role of SPOCK1 in proliferation, BrdU incorporation assay was performed in silenced cell lines (Figure 13A). SPOCK1 silencing decreased the ratio of the positive nuclei from 39.18% to 11.52% in HLE and from 18.67% to 10.28% in Huh7 cell lines compared to the control siRNA transfected cells (Figure 13B).

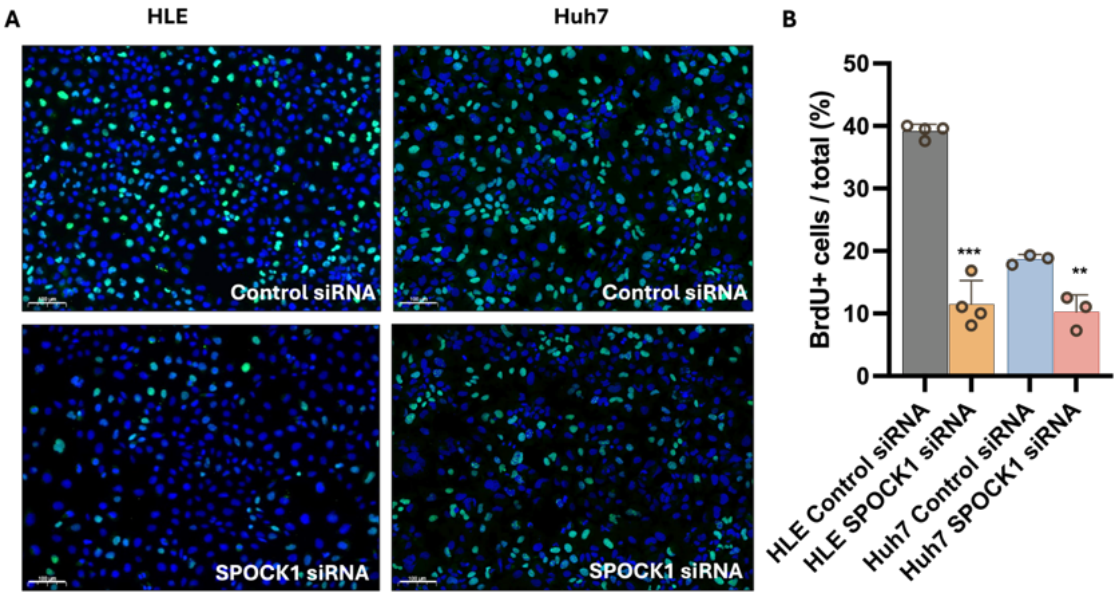

Figure 13. SPOCK1 silencing reduced the BrdU labeling index in human HLE and Huh7 cell lines. (A) Representative images of BrdU incorporation assay showed reduced number of labeled nuclei after SPOCK1 silencing. Blue: DAPI, green: BrdU (B) The BrdU labeling index was significantly reduced in SPOCK1 silenced cells. Data is presented as the mean ± SD, n>3/group. Statistical analysis was performed using unpaired t-test (94).

To further investigate the effect of SPOCK1 on HCC cells, a SPOCK1 expression vector was transfected in human HepG2 cell line, resulting in a 30.517-fold increase in SPOCK1 mRNA levels (Table 3). The intracellular protein level didn't change after the transfection, but increased levels of SPOCK1 were observed in the conditioned media (Figure 14A). We performed BrdU incorporation assay and overexpression of the SPOCK1 significantly increased the proportion of positive nuclei from 33.52% to 43.73% (Figure 14B, 14C).

Table 3. Upregulation of SPOCK1 mRNA after SPOCK1 plasmid transfection in HepG2 cell line.

Cell line	Relative quantification (fold change)	95% CI
HepG2	30.517	16.698-55.771

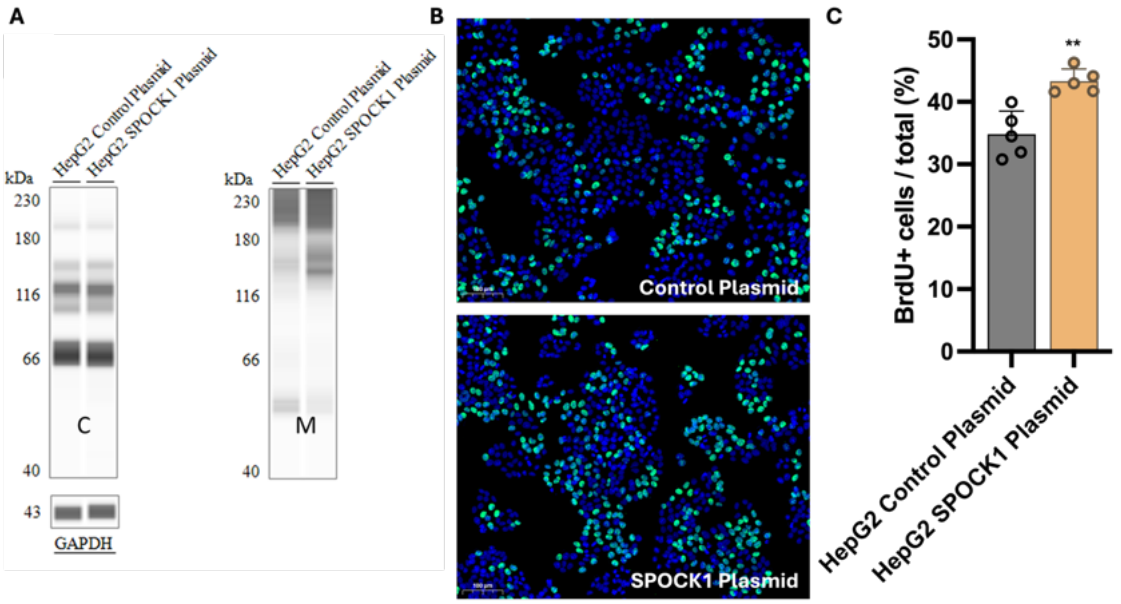

Figure 14. Overexpression of SPOCK1 in the human HepG2 cell line increased the level of secreted SPOCK1 and increased the BrdU labeling index. (A) SPOCK1 levels in intracellular and extracellular compartments measured by WES capillary electrophoresis. Overexpression of SPOCK1 resulted in an increase in the secreted level ("M") but not in the intracellular SPOCK1 level ("C"). (B)(C) Overexpression of SPOCK1 significantly increased the BrdU labeling index of the HepG2 cells as assessed by BrdU assay. Blue: DAPI, green: BrdU. Data is presented as the mean ± SD, n=5/group. Statistical analysis was performed using unpaired t-test (94).

4.9. Effect of SPOCK1 silencing on the signaling pathways

We used phospho-kinase array to analyze the changes in the activation/inhibition of signaling pathways following SPOCK1 silencing in HLE and Huh7 cell lines.

In both cell lines, significant decreases in phosphorylated EGFR, ERK1/2, TOR(S2448) and Yes levels were detected (Figure 15A, 15B). Phosphorylated MSK1/2, CREB, Src, Lyn, Fyn, Hck and Fgr levels were also decreased.

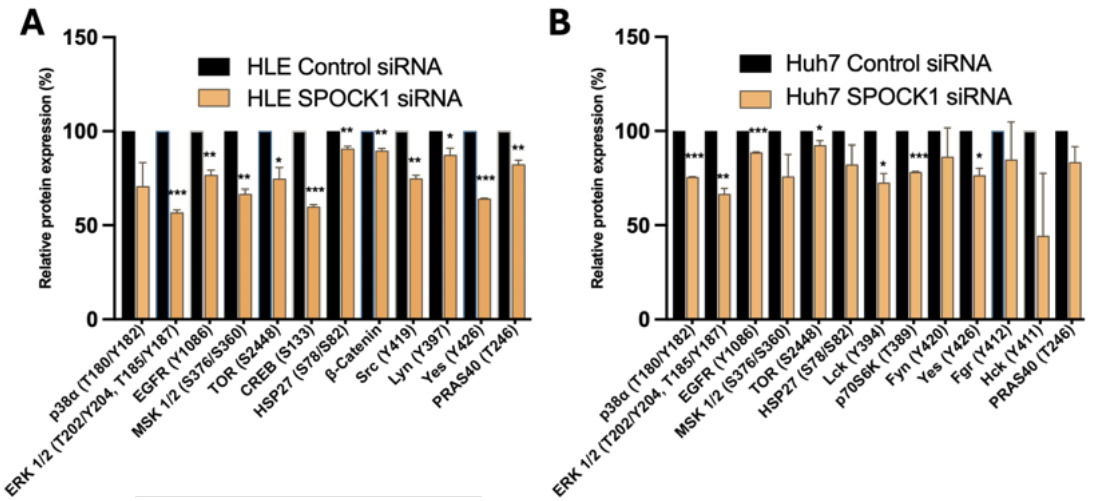

Figure 15. Signaling pathways associated with SPOCK1 in human HLE (A) and Huh7 (B) cell lines analyzed by phospho-kinase array. (A) SPOCK1 silencing significantly decreased the level of ERK 1/2 (T202/Y204, T185/Y187, EGFR (Y1086), MSK 1/2 (S376/S360), TOR (S2448), CREB (S133), HSP27 (S78/S82), β-Catenin, Src (Y419), Lyn (Y397), Yes (Y426), PRAS40 (T246) in HLE cell line and (B) the level of p38α (T180/Y182), ERK 1/2 (T202/Y204, T185/Y187, EGFR (Y1086), TOR (S2448), Yes (Y426), Lck (Y394), p70S6K (T389) in Huh7 cell line. Data is presented as the mean ± SD, n=2/group. Statistical analysis was performed using unpaired t-test (94).

5. Discussion

We have limited knowledge about the physiological function of SPOCK1, most of it being deducted from its structural homology with the members of the SPARC protein family.

We observed the expression of SPOCK1 in the arterial wall (smooth muscle cells), however, further research is required to ascertain its function. So far, one study has been published in this regard showing that SPOCK1 secreted by neurons can regulate vascular permeability of the blood-brain barrier in zebrafish by altering ECM, modifying the expression of cell junction genes and transcytosis in endothelial cells. Wild-type spock1 cells in the close proximity of blood vessels (10-20 μm) were able to rescue the leaky phenotype of spock1 mutant zebrafish. Similar observations were described in Spock1 knock out mice during the embryonal development, however, the blood brain barrier was fully restored in adult mice (98). The expression of SPOCK1 by smooth muscle cells in the arterial wall or perivascular hepatocytes raise the possibility of similar paracrine effect on liver endothelial cells.

The function of the hepatocytes depends on their localization in the parenchyma. Periportal hepatocytes preferentially express genes involved in gluconeogenesis, fatty acid metabolism and amino acid degradation, whereas pericentral hepatocytes express genes responsible for glycolysis, cholesterol production and xenobiotic metabolism. Markers related to these metabolic processes have been used to differentiate hepatocytes in different zones of the liver lobule. Glutamine synthetase is only expressed in pericentral hepatocytes in the normal liver (99), carbamoylphosphate synthase shows high expression in the periportal zone, cytochrome p450 (CYP450) IIE1 is preferentially expressed in the pericentral and midzonal region of the liver lobule (100,101). Interestingly, SPOCK1 expression was observed in both pericentral and periportal hepatocytes, with no positivity in the midzonal region. To the best of our knowledge, there is no marker with similar staining pattern, which raises interesting questions about the potential similarities in metabolic or other function.

Our experiments show co-localization of the mitochondrial marker MitoTracker and SPOCK1. Generally, CSPGs localize in the extracellular space, thus it is interesting that SPOCK1, which is dominated by CS GAGs, was found intracellularly. This may indicate its physiological function. The role of SPOCK1 in mitochondria is not known, one study

suggests its involvement in lipid metabolism trough regulation of the expression of another mitochondrial protein, UCP-1 (73). So far serglycin has been the only intracellular PG identified in mast cells granules and is involved in the storage of the proteases, histamine and serotonin (35).

Liver is well known for its high regenerative capacity. Hepatocyte proliferation during the regeneration is regulated by several factors. To determine whether SPOCK1 is involved in normal hepatocyte proliferation, we performed SPOCK1 IHC on explanted human liver samples after massive hepatic necrosis. We observed high expression of SPOCK1 in dedifferentiated hepatocytes organized into acinar structures. Previous studies found that these hepatocytes show focal positivity with AFP, Delta-like 1 homolog (DLK-1) and glypican-3 markers (10). Hepatocytes differentiating from ductular cells were also found to express SPOCK1. These cells show strong CYP-450 and HNF4 positivity and weak positivity for CK19, while they were not labelled with AFP, DLK-1 and Glypican-3 markers. At later stages these cells form round clusters of hepatocytes, interestingly faint SPOCK1 expression was observed in these regenerative foci. This raises the possibility that SPOCK1 plays a role in the early differentiation of the progenitor cells (10).

Contrary to previous published data (79) on the localization of SPOCK1 in hepatic stellate cells, we identified hepatocytes as the main source of SPOCK1 in liver cirrhosis and observed faint SPOCK1 positivity in fibroblasts. This is also supported by our in vitro experiment where isolated primary rat hepatocytes showed strong SPOCK1 expression but not the Lx2 hepatic stellate cell line (79). The lack of SPOCK1 positivity in the fibrotic areas also suggests that secreted SPOCK1 is released into the circulation rather than binding to the ECM.

We provided evidence that SPOCK1 is elevated in both cirrhosis and HCC. We observed a significant increase in SPOCK1 levels in in liver samples from HCV-infected patients with cirrhosis and HCC, as well as in cirrhotic liver samples of unknown etiology. The dominant GAG of SPOCK1 is CS, but it also carries HS sugar chains. It is well documented that HSPGs serve as docking sites for viruses. In the case of HCV, syndecan-1 and syndecan-4 serve as entry sites for the virus (102).

In HCCs, the GAG composition is shifted toward CSs. Here we show that concomitant with the downregulation of syndecan-1, we observed elevated SPOCK1 expression in the micro-metastases of the HCC. Glypican-3 and agrin are the dominant HSPGs in HCC, and versican has been considered as the primary source of the CS, however SPOCK1 may also contribute to this shift (33).

To overcome the limitations of the small sample size in our cohort, we further strengthened our results by analyzing publicly available databases. This supported our findings and revealed higher SPOCK1 mRNA expression in HCC samples compared to control samples. SPOCK1 levels were also significantly higher in HCC compared to the tumor surrounding area. Furthermore, high SPOCK1 expression in HCC correlated with significantly shorter overall survival. Our observation in HCC aligns with the literature where high SPOCK1 expression has been associated with poor prognosis in other cancer types (76,103).

The DEN-induced hepatocarcinogenesis model is widely used to investigate the development of liver cancer. DEN binds to the DNA and triggers mutations upon activation of cytochrome P450 enzymes. In our DEN injected mouse model, HCC reliably develops without preceding liver cirrhosis. We found upregulation of SPOCK1 expression during hepatocarcinogenesis. The upregulation of CHD1L detected at 9-months time-point could drive the changes seen in SPOCK1 levels. Our mouse model of hepatocarcinogenesis further supported that SPOCK1 is actively involved in HCC progression.

SPOCK1 also plays an important role in chemo- and targeted therapy and in the mechanism of resistance to these drugs. In a previous study we have shown that neoadjuvant chemotherapy in serous ovarian carcinoma significantly reduced SPOCK1 expression as assessed by IHC (103). By establishing Temozolomide resistant glioblastoma cell lines (U87 and U251) increased SPOCK1 expression was observed and these cells could be sensitized to Temozolomide by silencing SPOCK1 (104). Similar results have been observed in colon cancer cell lines (HCT116 and LoVo) by acquiring 5-fluorouracil resistance and in lung cancer cell lines (HCC827, PC9) resistant to third-generation EGFR tyrosine kinase inhibitor Osimertinib (105,106). On the other hand, generating Gefitinib-resistant PC9 NSCLC cell line harboring the T790M mutation

decreased the expression of the SPOCK1, thus sensitizing the cancer cell line to radiotherapy (107). Our cell culture experiments showed that HCC cell lines secreted SPOCK1 in conditioned medium. We therefore collected serum samples from HCC patients and measured SPOCK1 levels by ELISA. However, our cohort was relatively small, we detected elevated SPOCK1 levels in the serum of patients with HCC compared to control samples. This correlates with our previous findings where we detected increased level of SPOCK1 in serum from patients with serous ovarian carcinoma. Interestingly, we found that chemotherapy reduced the serum concentrations when compared to patients not receiving treatment (103). Li et al. performed transcriptome analysis of serum samples from patients with pT1 lung adenocarcinoma with or without lymph node metastasis. A series of transcripts, including SPOCK1, have been identified that reliably predict lymph node metastasis (108). Taken together, this data suggests that SPOCK1 is a promising candidate as a biomarker, easily accessible from liquid biopsy, that may help to monitor disease progression or the efficacy of therapy. However, the interpretation of increased levels requires caution, as elevated serum SPOCK1 levels have also been observed in sepsis and this correlated with the severity of the septic shock (88).

As expected, SPOCK1 promoted the BrdU incorporation of the HCC cell lines as measured by the BrdU incorporation assay. This finding aligns with previous studies that have emphasized the role of the SPOCK1 in proliferation and migration of various cancer cell lines (77,78,85,91,92,110,111). As a molecular background, we identified alterations in EGFR levels, members of MAPK signaling pathway (ERK1/2, MSK1/2, and CREB (S133)) and Src family kinases (SFKs) (Src, Lyn, and Yes, Fyn, Hck and Fgr), as a consequence of SPOCK1 silencing in HLE and Huh7 cell lines.

In vitro knocking in or knocking down of SPOCK1 didn’t affect intracellular levels of PG. This suggests that the secreted form plays a role in the observed changes in signaling pathways. The only reported receptor for SPOCK1 is integrin α5β1 (79), although the mechanistic details are not known.

Here we first reported that SPOCK1 regulates several members of SFKs, which are non-receptor tyrosine kinases that regulate different cellular functions. They are required for the disassembly and turnover of focal adhesions, thus regulating cell migration (112). They are also implicated in the activation of MMP2 and MMP9 in cancer cells (113,114).

They can be activated by direct binding to the cytoplasmic tails of integrin receptor beta1A, beta2, and beta3 (115). Guégan et al. have shown that activation of tyrosine kinase Yes can also promote HCC development. Hydrodynamic injection of activated Yes Y537F into mice was sufficient to induce tumor formation in a YAP/TAZ dependent manner (116). Together, these data suggest a possible link between SPOCK1 overexpression and activation of SFKs, and this promotes HCC.

In summary, our findings demonstrate that SPOCK1 is expressed in the arterial wall as well as in pericentral and periportal hepatocytes in the normal liver. We have also provided evidence for its mitochondrial localization. We identified high levels of SPOCK1 expression in the dedifferentiated hepatocytes during liver regeneration. Increased SPOCK1 expression was observed not only in HCC but also in cirrhosis and high SPOCK1 expression correlated with shorter overall survival. Elevated level of SPOCK1 was detected in the serum of HCC patients. SPOCK1 increased the BrdU labeling index in HCC cell lines and we identified members of the MAPKs and SFKs as being involved.

6. Conclusions

Our aim was to evaluate the role of the SPOCK1 in normal liver, regenerating liver, cirrhosis, and HCC. For this we evaluated the SPOCK1 expression in human and mouse liver samples, and measured its level in human serum samples. In addition, we assessed the effect of SPOCK1 on human HCC cell lines and analyzed the signaling pathways involved.

Based on our study, we conclude the following new findings:

1. In normal human liver, SPOCK1 is expressed in periportal and pericentral hepatocytes and in the smooth muscle cells of the arterial wall.
2. We identified the co-localization of SPOCK1 with mitochondria in cultured cells.
3. In human liver SPOCK1 shows a distinct expression pattern depending on the type of liver regeneration:
    a. It is highly expressed in the dedifferentiated hepatocytes.
    b. It is expressed in the differentiating cells with hepatocyte morphology derived from progenitor cells, however it is weakly expressed in the regenerative foci.
4. A significantly higher SPOCK1 expression was observed in HCV related human cirrhotic livers and HCC.
5. Higher SPOCK1 levels were detected in the serum samples of HCC patients.
6. Elevated SPOCK1 expression was observed in transformed foci in DEN-induced mouse hepatocarcinogenesis model.
7. Silencing SPOCK1 reduced the BrdU incorporation index of HCC cell lines (HLE and Huh7) and SPOCK1 overexpression increased the BrdU incorporation index of the HepG2 cell line.
8. Silencing SPOCK1 reduced the levels of SFK phosphoproteins.

7. Summary

SPOCK1 is a CSHS-PG that is overexpressed in several types of cancer and this correlates with poor prognosis. Under normal conditions it is highly expressed in certain regions of the brain, it has been also detected in the heart, skeletal muscle, prostate and testis, but not in the normal liver. It is also involved in the development of the blood-brain barrier and in the adipocyte differentiation and maturation. Its known transcription factor is CHD1L and it interact with the integrin α5β1 receptor. It is involved in the EMT, remodeling of the ECM trough activation of MMP2 and MMP9, and activates the AKT and Wnt/β-catenin signaling pathways.

Our objective was to investigate the role of SPOCK1 in physiological and pathological conditions of the liver.

We found that SPOCK1 is expressed in the hepatocytes adjacent to the portal and central veins in normal human liver and exhibits a cytoplasmic granular staining pattern. It co-localizes with mitochondrial markers on immunofluorescent staining. It is highly expressed in isolated primary rat hepatocytes but not in the Lx2 human hepatic stellate cell line in co-culture. High SPOCK1 expression was observed in dedifferentiated proliferating hepatocytes in human liver regeneration after massive hepatic necrosis. Its level was significantly increased in HCV-related cirrhosis and HCC and in silico analysis revealed that increased SPOCK1 expression in HCC correlated with shorter overall survival. Increased SPOCK1 and CHD1L expression was observed in the foci in DEN induced mouse model of hepatocarcinogenesis. We found that SPOCK1 is secreted into the culture medium of the HCC cell lines, and increased levels of SPOCK1 were also found in the serum of patients with HCC. Overexpression of SPOCK1 in HepG2 cell line increased the BrdU labeling index, whereas silencing of SPOCK1 in HLE and Huh7 cell lines decreased the BrdU labeling index. Phosphokinase array revealed that silencing SPOCK1 significantly decrease the level of EGFR, ERK1/2, TOR(S2448) and Yes in HLE and Huh7 cell lines.

SPOCK1 is present in the normal liver and its level is increased in liver regeneration also significantly increases in liver cirrhosis and HCC. Together with our in vitro data this suggest that SPOCK1 might contribute to the development and progression of HCC.

8. Reference

1. Bonnet F, Perin JP, Maillet P, Jolles P, Alliel PM. Characterization of a human seminal plasma glycosaminoglycan-bearing polypeptide. Biochem J. 1992 Dec 1;288(2):565–9.

2. Alliel PM, Perin J, Jollès P, Bonnet FJ. Testican, a multidomain testicular proteoglycan resembling modulators of cell social behaviour. Eur J Biochem. 1993 May;214(1):347–50.

3. Charbonnier F, Périn JP, Roussel G, Nussbaum JL, Alliel PM. [Cloning of testican/SPOCK in man and mouse. Neuromuscular expression perspectives in pathology]. C R Seances Soc Biol Fil. 1997;191(1):127–33.

4. Michalopoulos GK. Liver Regeneration. In: Arias IM, editor. The liver: biology and pathobiology. Sixth edition. Hoboken, NJ: Wiley-Blackwell; 2020. p. 566–84.

5. Michalopoulos GK. Hepatocytes of mice and men: Different regenerative signals? Hepatology [Internet]. 2023 Nov 16 [cited 2024 Oct 17]; Available from: https://journals.lww.com/10.1097/HEP.0000000000000693

6. Kim T, Mars WM, Stolz DB, Petersen BE, Michalopoulos GK. Extracellular matrix remodeling at the early stages of liver regeneration in the rat. Hepatology. 1997 Oct;26(4):896–904.

7. Michalopoulos GK, Bhushan B. Liver regeneration: biological and pathological mechanisms and implications. Nat Rev Gastroenterol Hepatol. 2021 Jan;18(1):40–55.

8. Gallai M, Sebestyén A, Nagy P, Kovalszky I, Ónody T, Thorgeirsson SS. Proteoglycan Gene Expression in Rat Liver after Partial Hepatectomy. Biochem Biophys Res Commun. 1996 Nov;228(3):690–4.

9. Yazici SE, Gedik ME, Leblebici CB, Kosemehmetoglu K, Gunaydin G, Dogrul AB. Can endocan serve as a molecular “hepatostat” in liver regeneration? Mol Med. 2023 Feb 27;29(1):29.

10. Dezső K, Nagy P, Paku S. Human liver regeneration following massive hepatic necrosis: Two distinct patterns. J Gastroenterol Hepatol. 2020 Jan;35(1):124–34.

11. Yoon SM, Gerasimidou D, Kuwahara R, Hytiroglou P, Yoo JE, Park YN, et al. Epithelial Cell Adhesion Molecule (EpCAM) Marks Hepatocytes Newly Derived from Stem/Progenitor Cells in Humans Δσ. Hepatology. 2011 Mar;53(3):964–73.

12. Itoh T, Miyajima A. Liver regeneration by stem/progenitor cells. Hepatology. 2014 Apr;59(4):1617–26.

13. World Heath Organization. International Agency for Research on Cancer. Incidence. [Internet]. [cited 2025 Mar 25]. Available from: https://gco.iarc.fr/today/en/dataviz/tables?mode=population&cancers=11&types=0

14. World Heath Organization. International Agency for Research on Cancer. Mortality. [Internet]. [cited 2025 Mar 25]. Available from: https://gco.iarc.fr/today/en/dataviz/tables?mode=population&cancers=11&types=1

15. Sung H, Ferlay J, Siegel RL, Laversanne M, Soerjomataram I, Jemal A, et al. Global Cancer Statistics 2020: GLOBOCAN Estimates of Incidence and Mortality Worldwide for 36 Cancers in 185 Countries. CA Cancer J Clin. 2021 May;71(3):209–49.

16. Singal AG, Kanwal F, Llovet JM. Global trends in hepatocellular carcinoma epidemiology: implications for screening, prevention and therapy. Nat Rev Clin Oncol. 2023 Dec;20(12):864–84.

17. Llovet JM, Kelley RK, Villanueva A, Singal AG, Pikarsky E, Roayaie S, et al. Hepatocellular carcinoma. Nat Rev Dis Primer. 2021 Jan 21;7(1):6.

18. Ginès P, Krag A, Abraldes JG, Solà E, Fabrellas N, Kamath PS. Liver cirrhosis. The Lancet. 2021 Oct;398(10308):1359–76.

19. Dezső K, Paku S, Kóbori L, Thorgeirsson SS, Nagy P. What Makes Cirrhosis Irreversible?—Consideration on Structural Changes. Front Med. 2022 Apr 27;9:876293.

20. Dezső K, Rókusz A, Bugyik E, Szücs A, Szuák A, Dorogi B, et al. Human liver regeneration in advanced cirrhosis is organized by the portal tree. J Hepatol. 2017 Apr;66(4):778–86.

21. Huang DQ, Singal AG, Kanwal F, Lampertico P, Buti M, Sirlin CB, et al. Hepatocellular carcinoma surveillance — utilization, barriers and the impact of changing aetiology. Nat Rev Gastroenterol Hepatol. 2023 Dec;20(12):797–809.

22. Sangro B, Argemi J, Ronot M, Paradis V, Meyer T, Mazzaferro V, et al. EASL Clinical Practice Guidelines on the management of hepatocellular carcinoma. J Hepatol. 2025 Feb;82(2):315–74.

23. Galle PR, Forner A, Llovet JM, Mazzaferro V, Piscaglia F, Raoul JL, et al. EASL Clinical Practice Guidelines: Management of hepatocellular carcinoma. J Hepatol. 2018 Jul;69(1):182–236.

24. Li L, Hu Y, Han J, Li Q, Peng C, Zhou J. Clinical Application of Liver Imaging Reporting and Data System for Characterizing Liver Neoplasms: A Meta-Analysis. Diagnostics. 2021 Feb 17;11(2):323.

25. Calderaro J, Ziol M, Paradis V, Zucman-Rossi J. Molecular and histological correlations in liver cancer. J Hepatol. 2019 Sep;71(3):616–30.

26. Calderaro J, Couchy G, Imbeaud S, Amaddeo G, Letouzé E, Blanc JF, et al. Histological subtypes of hepatocellular carcinoma are related to gene mutations and molecular tumour classification. J Hepatol. 2017 Oct;67(4):727–38.

27. Guichard C, Amaddeo G, Imbeaud S, Ladeiro Y, Pelletier L, Maad IB, et al. Integrated analysis of somatic mutations and focal copy-number changes identifies key genes and pathways in hepatocellular carcinoma. Nat Genet. 2012 Jun;44(6):694–8.

28. Ziol M, Poté N, Amaddeo G, Laurent A, Nault J, Oberti F, et al. Macrotrabecular-massive hepatocellular carcinoma: A distinctive histological subtype with clinical relevance. Hepatology. 2018 Jul;68(1):103–12.

29. Graham RP, Yeh MM, Lam-Himlin D, Roberts LR, Terracciano L, Cruise MW, et al. Molecular testing for the clinical diagnosis of fibrolamellar carcinoma. Mod Pathol. 2018 Jan;31(1):141–9.

30. Brown ZJ, Tsilimigras DI, Ruff SM, Mohseni A, Kamel IR, Cloyd JM, et al. Management of Hepatocellular Carcinoma: A Review. JAMA Surg. 2023 Apr 1;158(4):410.

31. Tabrizian P, Holzner ML, Mehta N, Halazun K, Agopian VG, Yao F, et al. Ten-Year Outcomes of Liver Transplant and Downstaging for Hepatocellular Carcinoma. JAMA Surg [Internet]. 2022 Jul 20 [cited 2024 Sep 24]; Available from: https://jamanetwork.com/journals/jamasurgery/fullarticle/2794451

32. Finn RS, Qin S, Ikeda M, Galle PR, Ducreux M, Kim TY, et al. Atezolizumab plus Bevacizumab in Unresectable Hepatocellular Carcinoma. N Engl J Med. 2020 May 14;382(20):1894–905.

33. Baghy K. Proteoglycans in liver cancer. World J Gastroenterol. 2016;22(1):379.

34. Casale J, Crane JS. Biochemistry, Glycosaminoglycans. In: StatPearls [Internet]. Treasure Island (FL): StatPearls Publishing; 2025 [cited 2025 Feb 13]. Available from: http://www.ncbi.nlm.nih.gov/books/NBK544295/

35. Iozzo RV, Schaefer L. Proteoglycan form and function: A comprehensive nomenclature of proteoglycans. Matrix Biol. 2015 Mar;42:11–55.

36. Theocharis AD, Karamanos NK. Proteoglycans remodeling in cancer: Underlying molecular mechanisms. Matrix Biol. 2019 Jan;75–76:220–59.

37. Dituri F, Gigante G, Scialpi R, Mancarella S, Fabregat I, Giannelli G. Proteoglycans in Cancer: Friends or Enemies? A Special Focus on Hepatocellular Carcinoma. Cancers. 2022 Jan;14(8):1902.

38. Barkovskaya A, Buffone A, Žídek M, Weaver VM. Proteoglycans as Mediators of Cancer Tissue Mechanics. Front Cell Dev Biol. 2020 Nov 30;8:569377.

39. Clausen TM, Sandoval DR, Spliid CB, Pihl J, Perrett HR, Painter CD, et al. SARS-CoV-2 Infection Depends on Cellular Heparan Sulfate and ACE2. Cell. 2020 Nov;183(4):1043-1057.e15.

40. Shi Q, Jiang J, Luo G. Syndecan-1 Serves as the Major Receptor for Attachment of Hepatitis C Virus to the Surfaces of Hepatocytes. J Virol. 2013 Jun 15;87(12):6866–75.

41. Kovalszky I, Pogany G, Molnar G, Jeney A, Lapis K, Karacsonyi S, et al. Altered glycosaminoglycan composition in reactive and neoplastic human liver. Biochem Biophys Res Commun. 1990 Mar;167(3):883–90.

42. Lv H, Yu G, Sun L, Zhang Z, Zhao X, Chai W. Elevate Level of Glycosaminoglycans and Altered Sulfation Pattern of Chondroitin Sulfate Are Associated with Differentiation Status and Histological Type of Human Primary Hepatic Carcinoma. Oncology. 2007;72(5–6):347–56.

43. Li HG. Clinicopathological significance of expression of paxillin, syndecan-1 and EMMPRIN in hepatocellular carcinoma. World J Gastroenterol. 2005;11(10):1445.

44. Reszegi A, Karászi K, Tóth G, Rada K, Váncza L, Turiák L, et al. Overexpression of Human Syndecan-1 Protects against the Diethylnitrosamine-Induced Hepatocarcinogenesis in Mice. Cancers. 2021 Mar 27;13(7):1548.

45. Hartmann U, Hülsmann H, Seul J, Röll S, Midani H, Breloy I, et al. Testican-3: a brain-specific proteoglycan member of the BM -40/ SPARC /osteonectin family. J Neurochem. 2013 May;125(3):399–409.

46. Vannahme C, Schübel S, Herud M, Gösling S, Hülsmann H, Paulsson M, et al. Molecular Cloning of Testican-2: Defining a Novel Calcium-Binding Proteoglycan Family Expressed in Brain. J Neurochem. 1999 Jul;73(1):12–20.

47. Schnepp A, Lindgren PK, Hülsmann H, Kröger S, Paulsson M, Hartmann U. Mouse Testican-2: EXPRESSION, GLYCOSYLATION, AND EFFECTS ON NEURITE OUTGROWTH. J Biol Chem. 2005 Mar;280(12):11274–80.

48. Nakada M, Yamada A, Takino T, Miyamori H, Takahashi T, Yamashita J, et al. Suppression of membrane-type 1 matrix metalloproteinase (MMP)-mediated MMP-2 activation and tumor invasion by testican 3 and its splicing variant gene product, N-Tes. Cancer Res. 2001 Dec 15;61(24):8896–902.

49. Charbonnier F, Périn JP, Mattei MG, Camuzat A, Bonnet F, Gressin L, et al. Genomic Organization of the Human SPOCK Gene and Its Chromosomal Localization to 5q31. Genomics. 1998 Mar;48(3):377–80.

50. Viloria K, Hill NJ. Embracing the complexity of matricellular proteins: the functional and clinical significance of splice variation. Biomol Concepts. 2016 May 1;7(2):117–32.

51. Viloria K, Munasinghe A, Asher S, Bogyere R, Jones L, Hill NJ. A holistic approach to dissecting SPARC family protein complexity reveals FSTL-1 as an inhibitor of pancreatic cancer cell growth. Sci Rep. 2016 Nov 25;6(1):37839.

52. Li MY, Gao RP, Zhu Q, Chen Y, Tao BB, Zhu YC. Skeletal muscle-derived FSTL1 starting up angiogenesis by regulating endothelial junction via activating Src pathway can

be upregulated by hydrogen sulfide. Am J Physiol-Cell Physiol. 2023 Nov 1;325(5):C1252–66.

53. Lau C, Poon R, Cheung S, Yu W, Fan S. SPARC and Hevin expression correlate with tumour angiogenesis in hepatocellular carcinoma. J Pathol. 2006 Dec;210(4):459–68.

54. Bradshaw AD. Diverse biological functions of the SPARC family of proteins. Int J Biochem Cell Biol. 2012 Mar;44(3):480–8.

55. Marr HS, Edgell CJS. Testican-1 inhibits attachment of Neuro-2a cells. Matrix Biol. 2003 May;22(3):259–66.

56. BaSalamah MAM, Marr HS, Duncan AW, Edgell CJS. Testican in Human Blood1. Biochem Biophys Res Commun. 2001 May;283(5):1083–90.

57. Stark M, Danielsson O, Griffiths WJ, Jörnvall H, Johansson J. Peptide repertoire of human cerebrospinal fluid: novel proteolytic fragments of neuroendocrine proteins. J Chromatogr B Biomed Sci App. 2001 Apr;754(2):357–67.

58. Edgell CJS, BaSalamah MA, Marr HS. Testican-1: A Differentially Expressed Proteoglycan with Protease Inhibiting Activities. Int Rev Cytol. 2004;236:101–22.

59. Hohenester E, Maurer P, Hohenadl C, Timpl R, Jansonius JN, Engel J. Structure of a novel extracellular Ca2+-binding module in BM-40. Nat Struct Biol. 1996 Jan;3(1):67–73.

60. Kohfeldt E, Maurer P, Vannahme C, Timpl R. Properties of the extracellular calcium binding module of the proteoglycan testican. FEBS Lett. 1997 Sep 15;414(3):557–61.

61. Bocock JP, Edgell CS, Marr HS, Erickson AH. Human proteoglycan testican-1 inhibits the lysosomal cysteine protease cathepsin L. Eur J Biochem. 2003 Oct;270(19):4008–15.

62. Molina F, Bouanani M, Pau B, Granier C. Characterization of the Type-1 Repeat from Thyroglobulin, a Cysteine-Rich Module Found in Proteins from Different Families. Eur J Biochem. 1996 Aug;240(1):125–33.

63. Sammon D, Krueger A, Busse-Wicher M, Morgan RM, Haslam SM, Schumann B, et al. Molecular mechanism of decision-making in glycosaminoglycan biosynthesis. Nat Commun. 2023 Oct 13;14(1):6425.

64. Varadi M, Bertoni D, Magana P, Paramval U, Pidruchna I, Radhakrishnan M, et al. AlphaFold Protein Structure Database in 2024: providing structure coverage for over 214 million protein sequences. Nucleic Acids Res. 2024 Jan 5;52(D1):D368–75.

65. Jumper J, Evans R, Pritzel A, Green T, Figurnov M, Ronneberger O, et al. Highly accurate protein structure prediction with AlphaFold. Nature. 2021 Aug 26;596(7873):583–9.

66. Bonnet F, Périn JP, Charbonnier F, Camuzat A, Roussel G, Nussbaum JL, et al. Structure and Cellular Distribution of Mouse Brain Testican. J Biol Chem. 1996 Feb;271(8):4373–80.

67. Marr HS, Basalamah MA, Bouldin TW, Duncan AW, Edgell CJS. Distribution of testican expression in human brain. Cell Tissue Res. 2000 Nov 6;302(2):139–44.

68. Marr HS, Basalamah MA, Edgell CJS. Endothelial Cell Expression of Testican mRNA. Endothelium. 1997 Jan;5(3):209–19.

69. Charbonnier F, Chanoine C, Cifuentes-Diaz C, Gallien CL, Rieger F, Alliel PM, et al. Expression of the proteoglycan SPOCK during mouse embryo development. Mech Dev. 2000 Feb;90(2):317–21.

70. Röll S, Seul J, Paulsson M, Hartmann U. Testican-1 is dispensable for mouse development. Matrix Biol. 2006 Aug;25(6):373–81.

71. Iseki K, Hagino S, Zhang Y, Mori T, Sato N, Yokoya S, et al. Altered expression pattern of testican-1 mRNA after brain injury. Biomed Res. 2011;32(6):373–8.

72. Zhong J, Krawczyk SA, Chaerkady R, Huang H, Goel R, Bader JS, et al. Temporal Profiling of the Secretome during Adipogenesis in Humans. J Proteome Res. 2010 Oct 1;9(10):5228–38.

73. Alshargabi R, Shinjo T, Iwashita M, Yamashita A, Sano T, Nishimura Y, et al. SPOCK1 induces adipose tissue maturation: New insights into the function of SPOCK1 in metabolism. Biochem Biophys Res Commun. 2020 Dec;533(4):1076–82.

74. Dhamija R, Graham JM, Smaoui N, Thorland E, Kirmani S. Novel de novo SPOCK1 mutation in a proband with developmental delay, microcephaly and agenesis of corpus callosum. Eur J Med Genet. 2014 Mar;57(4):181–4.

75. Cui X, Wang Y, Lan W, Wang S, Cui Y, Zhang X, et al. SPOCK1 promotes metastasis in pancreatic cancer via NF-κB-dependent epithelial-mesenchymal transition by interacting with IκB-α. Cell Oncol. 2022 Feb;45(1):69–84.

76. Han J, Rong Y, Gao X. Multiomic analysis of the function of *SPOCK1* across cancers: an integrated bioinformatics approach. J Int Med Res. 2021 Jun;49(6):030006052096265.

77. Chen D, Zhou H, Liu G, Zhao Y, Cao G, Liu Q. SPOCK 1 promotes the invasion and metastasis of gastric cancer through Slug-induced epithelial-mesenchymal transition. J Cell Mol Med. 2018 Feb;22(2):797–807.

78. Li Y, Chen L, Chan THM, Liu M, Kong K, Qiu J, et al. SPOCK1 Is Regulated by CHD1L and Blocks Apoptosis and Promotes HCC Cell Invasiveness and Metastasis in Mice. Gastroenterology. 2013 Jan;144(1):179-191.e4.

79. Du Z, Lin Z, Wang Z, Liu D, Tian D, Xia L. SPOCK1 overexpression induced by platelet-derived growth factor-BB promotes hepatic stellate cell activation and liver fibrosis through the integrin α5β1/PI3K/Akt signaling pathway. Lab Invest. 2020 Aug;100(8):1042–56.

80. Xiong X, Lai X, Li A, Liu Z, Ma N. Diversity roles of CHD1L in normal cell function and tumorigenesis. Biomark Res. 2021 Dec;9(1):16.

81. Stemmler MP, Eccles RL, Brabletz S, Brabletz T. Non-redundant functions of EMT transcription factors. Nat Cell Biol. 2019 Jan;21(1):102–12.

82. Sun L rui, Li S yu, Guo Q shi, Zhou W, Zhang H mei. SPOCK1 Involvement in Epithelial-to-Mesenchymal Transition: A New Target in Cancer Therapy? Cancer Manag Res. 2020 May;Volume 12:3561–9.

83. Miao L, Wang Y, Xia H, Yao C, Cai H, Song Y. SPOCK1 is a novel transforming growth factor-β target gene that regulates lung cancer cell epithelial-mesenchymal transition. Biochem Biophys Res Commun. 2013 Nov;440(4):792–7.

84. Veenstra VL, Damhofer H, Waasdorp C, Steins A, Kocher HM, Medema JP, et al. Stromal SPOCK 1 supports invasive pancreatic cancer growth. Mol Oncol. 2017 Aug;11(8):1050–64.

85. Liu Y, Han T, Wu J, Zhou J, Guo J, Miao R, et al. SPOCK1, as a potential prognostic and therapeutic biomarker for lung adenocarcinoma, is associated with epithelial-mesenchymal transition and immune evasion. J Transl Med. 2023 Dec 12;21(1):909.

86. Fan LC, Jeng YM, Lu YT, Lien HC. SPOCK1 Is a Novel Transforming Growth Factor-β–Induced Myoepithelial Marker That Enhances Invasion and Correlates with Poor Prognosis in Breast Cancer. Castresana JS, editor. PLOS ONE. 2016 Sep 14;11(9):e0162933.

87. Alshargabi R, Sano T, Yamashita A, Takano A, Sanada T, Iwashita M, et al. SPOCK1 is a novel inducer of epithelial to mesenchymal transition in drug-induced gingival overgrowth. Sci Rep. 2020 Jun 17;10(1):9785.

88. Chien MH, Lin YW, Wen YC, Yang YC, Hsiao M, Chang JL, et al. Targeting the SPOCK1-snail/slug axis-mediated epithelial-to-mesenchymal transition by apigenin contributes to repression of prostate cancer metastasis. J Exp Clin Cancer Res. 2019 Dec;38(1):246.

89. Lin YW, Wen YC, Hsiao CH, Lai FR, Yang SF, Yang YC, et al. Proteoglycan SPOCK1 as a Poor Prognostic Marker Promotes Malignant Progression of Clear Cell Renal Cell Carcinoma via Triggering the Snail/Slug-MMP-2 Axis-Mediated Epithelial-to-Mesenchymal Transition. Cells. 2023 Jan 17;12(3):352.

90. Berger EA, McClellan SA, Barrett RP, Hazlett LD. Testican-1 Promotes Resistance against *Pseudomonas aeruginosa* –Induced Keratitis through Regulation of MMP-2 Expression and Activation. Investig Opthalmology Vis Sci. 2011 Jul 18;52(8):5339.

91. Yang J, Yang Q, Yu J, Li X, Yu S, Zhang X. SPOCK1 promotes the proliferation, migration and invasion of glioma cells through PI3K/AKT and Wnt/β-catenin signaling pathways. Oncol Rep. 2016 Jun;35(6):3566–76.

92. Wang T, Liu X, Tian Q, Liang T, Chang P. Reduced SPOCK1 expression inhibits non-small cell lung cancer cell proliferation and migration through Wnt/β-catenin signaling. Eur Rev Med Pharmacol Sci. 2018 Feb;22(3):637–44.

93. Zhao P, Guan HT, Dai ZJ, Ma YG, Liu XX, Wang XJ. Knockdown of SPOCK1 Inhibits the Proliferation and Invasion in Colorectal Cancer Cells by Suppressing the PI3K/Akt Pathway. Oncol Res Featur Preclin Clin Cancer Ther. 2016 Oct 27;24(6):437–45.

94. Váncza L, Karászi K, Péterfia B, Turiák L, Dezső K, Sebestyén A, et al. SPOCK1 Promotes the Development of Hepatocellular Carcinoma. Front Oncol. 2022 Feb 3;12:819883.

95. Váncza L, Tátrai P, Reszegi A, Baghy K, Kovalszky I. SPOCK1 with unexpected function. The start of a new career. Am J Physiol-Cell Physiol. 2022 Apr 1;322(4):C688–93.

96. Menyhárt O, Nagy Á, Győrffy B. Determining consistent prognostic biomarkers of overall survival and vascular invasion in hepatocellular carcinoma. R Soc Open Sci. 2018 Dec;5(12):181006.

97. Goldfarb S, Pugh TD, Koen H, He YZ. Preneoplastic and neoplastic progression during hepatocarcinogenesis in mice injected with diethylnitrosamine in infancy. Environ Health Perspect. 1983 Apr;50:149–61.

98. O'Brown NM, Patel NB, Hartmann U, Klein AM, Gu C, Megason SG. The secreted neuronal signal Spock1 promotes blood-brain barrier development. Dev Cell. 2023 Sep;58(17):1534-1547.e6.

99. Paris J, Henderson NC. Liver zonation, revisited. Hepatology. 2022 Oct;76(4):1219–30.

100. Wagenaar GTM, Geerts WJC, Chamuleau RAFM, Deutz NEP, Lamers WH. Lobular patterns of expression and enzyme activities of glutamine synthase, carbamoylphosphate synthase and glutamate dehydrogenase during postnatal development of the porcine liver. Biochim Biophys Acta BBA - Gen Subj. 1994 Aug;1200(3):265–70.

101. Dezsõ K, Papp V, Bugyik E, Hegyesi H, Sáfrány G, Bödör C, et al. Structural analysis of oval-cell–mediated liver regeneration in rats. Hepatology. 2012 Oct;56(4):1457–67.

102. Xu Y, Martinez P, Séron K, Luo G, Allain F, Dubuisson J, et al. Characterization of Hepatitis C Virus Interaction with Heparan Sulfate Proteoglycans. Diamond MS, editor. J Virol. 2015 Apr;89(7):3846–58.

103. Váncza L, Horváth A, Seungyeon L, Rókusz A, Dezső K, Reszegi A, et al. SPOCK1 Overexpression Suggests Poor Prognosis of Ovarian Cancer. Cancers. 2023 Mar 29;15(7):2037.

104. Yu F, Li G, Gao J, Sun Y, Liu P, Gao H, et al. SPOCK1 is upregulated in recurrent glioblastoma and contributes to metastasis and Temozolomide resistance. Cell Prolif. 2016 Apr;49(2):195–206.

105. Qu YL, Liu XL, Zhao SY, Zhai XF. SPOCK1 silencing decreases 5-FU resistance through PRRX1 in colorectal cancer. Pathol - Res Pract. 2022 Jun;234:153895.

106. Gao Y, Yu M, Ma M, Zhuang Y, Qiu X, Zhao Q, et al. SPOCK1 contributes to the third-generation EGFR tyrosine kinase inhibitors resistance in lung cancer. J Cell Biochem. 2019 Aug;120(8):12566–73.

107. Xu Y, Zhao P, Xu X, Zhang S, Xia B, Zhu L. T790M mutation sensitizes non-small cell lung cancer cells to radiation via suppressing SPOCK1. Biochem Biophys Rep. 2024 Jul;38:101729.

108. Li X, Gu Y, Hu B, Shao M, Li H. A liquid biopsy assay for the noninvasive detection of lymph node metastases in T1 lung adenocarcinoma. Thorac Cancer. 2024 Apr 29;1759-7714.15315.

109. Lee Y, Lee W, Chang H, Kim S, Kim J, Bae J. Testican-1, as a novel diagnosis of sepsis. J Cell Biochem. 2018 May;119(5):4216–23.

110. Shu YJ, Weng H, Ye YY, Hu YP, Bao RF, Cao Y, et al. SPOCK1 as a potential cancer prognostic marker promotes the proliferation and metastasis of gallbladder cancer cells by activating the PI3K/AKT pathway. Mol Cancer. 2015 Dec;14(1):12.

111. Wang Z, Yao Y ting, Xu H, Chen Y bo, Gu M, Cai Z kang, et al. SPOCK1 promotes tumor growth and metastasis in human prostate cancer. Drug Des Devel Ther. 2016 Jul;Volume 10:2311–21.

112. Webb DJ, Donais K, Whitmore LA, Thomas SM, Turner CE, Parsons JT, et al. FAK–Src signalling through paxillin, ERK and MLCK regulates adhesion disassembly. Nat Cell Biol. 2004 Feb;6(2):154–61.

113. Sánchez-Pozo J, Baker-Williams AJ, Woodford MR, Bullard R, Wei B, Mollapour M, et al. Extracellular Phosphorylation of TIMP-2 by Secreted c-Src Tyrosine Kinase Controls MMP-2 Activity. iScience. 2018 Mar;1:87–96.

114. Cortesreynosa P, Robledo T, Maciassilva M, Wu S, Salazar E. Src kinase regulates metalloproteinase-9 secretion induced by type IV collagen in MCF-7 human breast cancer cells. Matrix Biol. 2008 Apr;27(3):220–31.

115. Arias-Salgado EG, Lizano S, Sarkar S, Brugge JS, Ginsberg MH, Shattil SJ. Src kinase activation by direct interaction with the integrin β cytoplasmic domain. Proc Natl Acad Sci. 2003 Nov 11;100(23):13298–302.

116. Guégan JP, Lapouge M, Voisin L, Saba-El-Leil MK, Tanguay PL, Lévesque K, et al. Signaling by the tyrosine kinase Yes promotes liver cancer development. Sci Signal. 2022 Jan 18;15(717):eabj4743.

9. Bibliography of the candidate's publications

9.1. Related to the thesis

1. **Váncza, L.**; Tátrai, P.; Reszegi, A.; Baghy, K.; Kovalszky, I.

SPOCK1 with unexpected function. The start of a new career

AMERICAN JOURNAL OF PHYSIOLOGY: CELL PHYSIOLOGY 322: 4 pp. C688 C693. (2022)

Összefoglaló cikk (Folyóiratcikk) IF: -

2. **Váncza, L.**; Karászi, K.; Péterfia, B.; Turiák, L.; Dezső, K.; Sebestyén, A.; Reszegi, A.; Petővári, G.; Kiss, A.; Schaff, Zs.; Baghy, K.; Kovalszky, I.

SPOCK1 Promotes the Development of Hepatocellular Carcinoma

FRONTIERS IN ONCOLOGY 12 Paper: 819883 , 18 p. (2022)

Szakcikk (Folyóiratcikk)

IF: 4,7

3. **Váncza, L.**; Karászi, K.; Péterfia, B.; Turiák, L.; Dezső, K.; Sebestyén, A.; Reszegi, A.; Petővári, G.; Kiss, A.; Schaff, Zs.; Baghy, K.; Kovalszky, I.

Corrigendum: SPOCK1 promotes the development of hepatocellular carcinoma

FRONTIERS IN ONCOLOGY 13 Paper: 1203745 , 1 p. (2023)

Hozzászólás, helyreigazítás (Folyóiratcikk)

IF: -

9.2. Related to the topic

1. **Váncza, L.**; Horváth, A.*; Seungyeon, L.*; Rókusz, A.; Dezső, K.; Reszegi, A.; Petővári, G.; Götte, M.; Kovalszky, I.; Baghy, K.

SPOCK1 Overexpression Suggests Poor Prognosis of Ovarian Cancer

CANCERS 15 : 7 Paper: 2037 , 19 p. (2023)

Szakcikk (Folyóiratcikk)

*Megosztott első szerzőség

IF: 4,5

9.3. Not related to the topic

1. Hollósi, P.; **Váncza, L.***; Karászi, K.*; Dobos, K.; Péterfia, B.; Tátrai, E.; Tátrai, P.; Szarvas, T.; Paku, S.; Szilák, L.; Kovalszky, I.

Syndecan-1 Promotes Hepatocyte-Like Differentiation of Hepatoma Cells Targeting Ets-1 and AP-1

BIOMOLECULES 10 : 10 Paper: 1356 , 25 p. (2020)

Szakcikk (Folyóiratcikk)

*Megosztott első szerzőség

IF: 4,879

2. Reszegi, A.; Karászi, K.*; Tóth, G.*; Rada, K.; **Váncza, L**.; Turiák, L.; Schaff, Zs.; Kiss, A.; Szilák, L.; Szabó, G.; Petővári, G.; Sebestyén, A.; Dezső, K.; Regős, E.; Tátrai, P.; Baghy, K.; Kovalszky, I.

Overexpression of Human Syndecan-1 Protects against the Diethylnitrosamine-Induced Hepatocarcinogenesis in Mice

CANCERS 13 : 7 Paper: 1548 , 33 p. (2021)

Szakcikk (Folyóiratcikk)

IF: 6,575

3. **Váncza, L.**; Torok, N.J.

Primary sclerosing cholangitis and the path to translation

JOURNAL OF CLINICAL INVESTIGATION 133 : 17 Paper: 174218 (2023)

Rövid közlemény (Folyóiratcikk)

IF: 13,3

4. Li, Y.; Jiang, J.X.; Fan, W.; Fish, S.R.; Das, S.; Gupta, P.; Mozes, G.; **Váncza, L.**; Sarkar, S.; Kunimoto, K.; Chen D.; Park H.; Clemens D.; Tomilov A.; Cortopassi G. ; Török N.J.

Shc Is Implicated in Calreticulin-Mediated Sterile Inflammation in Alcoholic Hepatitis

CELLULAR AND MOLECULAR GASTROENTEROLOGY AND HEPATOLOGY 15 : 1 pp. 197-211. , 15 p. (2023)

Szakcikk (Folyóiratcikk)

IF: 7,1

5. Li, Y.; Fan, W.; Lo, T.; Jiang, J.; Fish, S.; Tomilov, A.; Chronopoulos, A.; Bansal, V.; Mozes, G.; **Váncza, L.**; Kunimoto K.; Ye J.; Becker L.; Das S.; Park H.; Wei Yi; Ranjbarvaziri S.; Bernstein D.; Ramsey J.; Cortopassi G.; Török N. J.

P46Shc inhibits mitochondrial ACAA2 thiolase, exacerbating mitochondrial injury and inflammation in aging livers

AMERICAN JOURNAL OF PATHOLOGY In press p. In press (2024)

Szakcikk (Folyóiratcikk)

IF: 4,7

6. Fan, W.; Adebowale, K.; **Váncza, L.**; Li, Y.; Rabbi, Md F.; Kunimoto, K.; Chen, D.; Mozes, G.; Chiu, D. K.; Li, Y.; Tao J.; Wei Y.; Adeniji N.; Brunsing R. L.; Dhanasekaran R.; Singhi A.; Geller D.; Lo S. H.; Hodgson L.; Engleman E. G.; Charville G. W.; Charu V.; Monga S. P.; Kim T.; Wells R. G.; Chaudhuri O. ; Torok N. J.

Matrix viscoelasticity promotes liver cancer progression in the pre-cirrhotic liver

NATURE 626 : 7999 pp. 635-642. , 18 p. (2024)

Szakcikk (Folyóiratcikk)

IF: 50,5

7. Bárdos, D.; Szakadáti, H. ; **Váncza, L**.; Drácz, B.; Dezső, K.; Baghy, K.; Szijártó, A.; Kovalszky, I.; Werling, K.

A SPOCK1 fehérje szerepe a máj egészséges és kóros működéseiben

ORVOSI HETILAP 166 : 3 pp. 82-89. , 8 p. (2025)

Összefoglaló cikk (Folyóiratcikk)

IF: -

10. Acknowledgements

Ennek a dolgozatnak a megszületését rengeteg ember segítette, akiknek itt néhány sorban (bár többet érdemelnének) szeretném kifejezni a hálámat és megköszönni a támogatásukat.

Hálával tartozom Dr. Matolcsy András professzornak, hogy a Semmelweis Egyetem Patológiai és Kísérleti Rákkutató Intézetben lehetőséget adott arra, hogy tudományos munkát végezhessek.

Köszönöm Dr. Kovalszky Ilona professzorasszonynak, aki már tudományos diákköri hallgatóként befogadott laborjába. Kutatás iránti szenvedélye, lelkesedése inspiráló volt, tudását önzetlenül megosztotta. Laborjában családtagnak érezhettem magam.

Köszönöm Dr. Dezső Katalin professzorasszonynak szakmai iránymutatását, hogy tudását és tapasztalatát megosztotta. Köszönöm, hogy a kérdéseimre mindig megoldást jelentett, támogatott döntéseimben. Köszönöm példamutatását, szakma iránti elhivatottságát, melyre törekedni fogok.

Köszönöm Andinak és Katának, Krisztinek és Krisztának az oktatást, szakmai támogatást, segítségét és családias hangulatot.

Köszönöm a szüleimnek, Évának és Jánosnak a sok áldozatot, lemondást, amit a taníttatásomért hoztak. Köszönöm, hogy példaként szolgáltak, alázatra neveltek és hogy egy biztos hátteret adtak, ahova a legnehezebb időszakokban is fordulhattam.

Köszönöm Katának, Máténak, Péternek, Csillának és Mátyásnak, hogy végig mellettem voltak, mosolyt csaltak az arcomra.

Köszönöm Imolának a szeretetét, támogatását és a sok nevetést; hogy minden helyzetben megmutatja az élet napos oldalát.

Köszönöm Villőnek, Kingának és Barninak, hogy a nehéz döntésekben mellettem voltak és otthon helyett otthont adtak.

Köszönöm Manunak és Manónak a kellemes légkört, amelyet a laborban biztosítottak, és a sok nevetést ami erőt adott a mindennapokban.